Contrôle actif des vibrations dans des structures mécaniques minces instrumentées de transducteurs piézoélectriques

Sami TLIBA

Laboratoire Signaux & Systèmes (L2S)
Université Paris-Saclay, Faculté des Sciences d'Orsay
CNRS
CentraleSupélec

CTIP 2023 – Control Theory & Inverse Problems

8-10 mai 2023, Monastir, Tunisie

Introduction

Fonctionnement des moteurs, phases d'apportage :

- Chocs, déformations dynamiques $\Rightarrow$ **Vibrations**
- Dégradation des équipements embarqués

Atténuation nécessaire, 2 approches

- Passive : raidisseurs mécaniques
- Active : Contrôle actif des vibrations

DGA – THALES AS

Structures intelligentes

Introduction

Cahier des charges industriel :

- Amortir les pics de résonance des modes gênants
- Garantir la stabilité du système
- Approche active : industrialisable
  - Légère
  - Source d'énergie disponible
  - Implémentation
  - Retouche

DGA – THALES AS

Sommaire

1. **Objectifs**
   - Structures intelligentes
   - Approche générique pour le contrôle actif des vibrations
2. **Modélisation d'une structure intelligente**
   - Formulation du problème
   - Approche éléments finis
3. **Mise en œuvre expérimentale**
4. **Commande robuste pour le contrôle actif des vibrations**
   - Mise en forme du problème de commande
   - Synthèse, analyse et résultats expérimentaux
5. **Prospectives : commande à retard, correcteur QPB-MID**

Objectifs

Aborder les problèmes posés par les structures intelligentes :

- Introduction au structures dites « intelligentes »
  - ➔ Caractérisation physique du matériau actif
  - ➔ Fonction capteur/actionneur sur une structure mince de type plaque
  - ➔ Présentation des supports expérimentaux
- Problème du placement optimal des instruments (capteurs/actionneurs)
  - ➔ Choix d’un critère d’optimisation
  - ➔ Dimensionnement des transducteurs
- Choix d’une stratégie d’étude

Objectifs

Proposer une approche générique pour le contrôle actif des vibrations :

- Obtention d'un modèle dynamique
  - ➔ Entrée – sortie
  - ➔ Linéaire & dimension finie
  - ➔ Bande de fréquence : [0 – 2000 Hz]
- Synthèse d'une loi de commande
  - ➔ Cahier des charges multiobjectif
  - ➔ Correcteur à structure figée : retour de sortie dynamique, réduite
- Finalité : Mise en œuvre expérimentale

Structures intelligentes

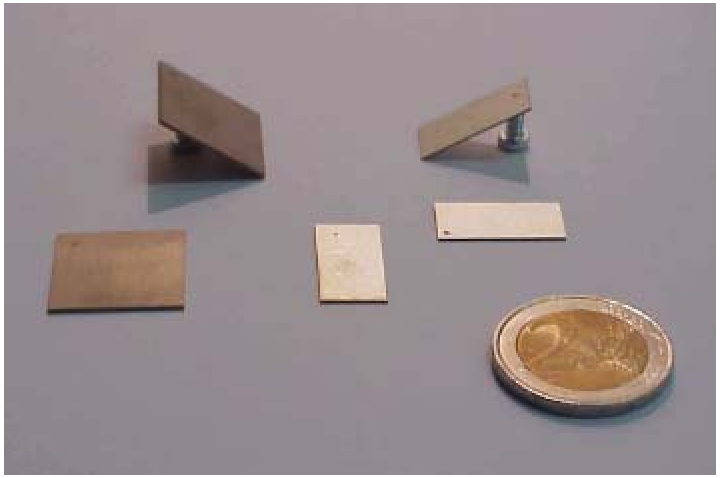

Matériau actif : pastilles piézoélectriques

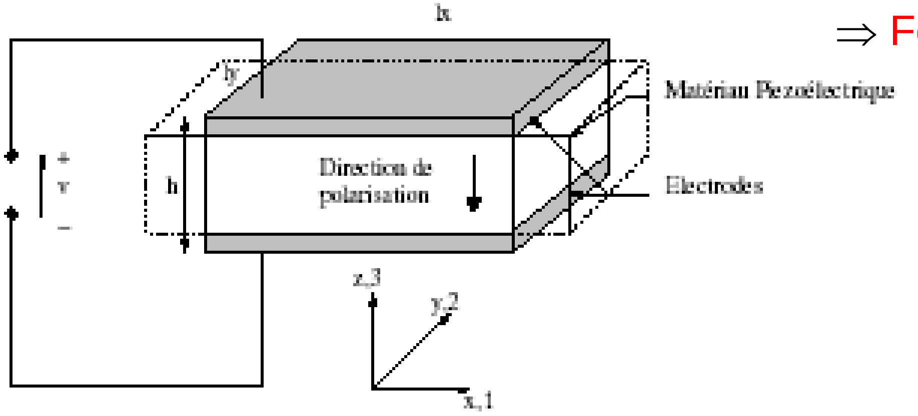

Effet piézoélectrique directe :

Apparition d'une déformation sous l'effet d'un champ électrique : dilatation/compression

$\Rightarrow$ Fonction actionneur

Effet piézoélectrique inverse :

Apparition d'une différence de potentiel sous l'effet d'une déformation mécanique

$\Rightarrow$ Fonction capteur

Structures intelligentes

Relations de comportement (Fonctionnement linéaire, pas d'hystérésis)

Couple de variables choisi	Equations de comportement
$(\boldsymbol{\sigma}, \overrightarrow{E})$	$\overrightarrow{D} = [d]\boldsymbol{\sigma} + [\epsilon^{\sigma}]\overrightarrow{E}$ $\boldsymbol{\varepsilon} = [s^{E}]\boldsymbol{\sigma} + [d]^{T}\overrightarrow{E}$
$(\boldsymbol{\sigma}, \overrightarrow{D})$	$\overrightarrow{E} = -[g]\boldsymbol{\sigma} + [\epsilon^{\sigma}]^{-1}\overrightarrow{D}$ $\boldsymbol{\varepsilon} = [s^{D}]\boldsymbol{\sigma} + [g]^{T}\overrightarrow{D}$
$(\boldsymbol{\varepsilon}, \overrightarrow{E})$	$\overrightarrow{D} = [e]\boldsymbol{\varepsilon} + [\epsilon^{\varepsilon}]\overrightarrow{E}$ $\boldsymbol{\sigma} = [c^{E}]\boldsymbol{\varepsilon} - [e]^{T}\overrightarrow{E}$
$(\boldsymbol{\varepsilon}, \overrightarrow{D})$	$\overrightarrow{E} = -[h]\boldsymbol{\varepsilon} + [\epsilon^{\varepsilon}]^{-1}\overrightarrow{D}$ $\boldsymbol{\sigma} = [c^{D}]\boldsymbol{\varepsilon} - [h]^{T}\overrightarrow{D}$

Structures intelligentes

Notations et signification physique des paramètres :

Constantes piézoélectriques :

$[d]$ = Constante de charge (matrice 3×6) en $C.N^{-1}$

$[g]$ = Constante de tension en $V.m.N^{-1}$ ou $m^2.C^{-1}$

$[e]$ = Constante en $N.V^{-1}m^{-1}$ ou $C.m^{-2}$

$[h]$ = Constante en $N.C^{-1}$ ou $V.m^{-1}$

Constantes diélectriques (relatives à la permittivité diélectrique du vide $\epsilon_0 = \frac{1}{36\pi\, 10^9}$) :

$[\epsilon^\sigma]$ = permittivité diélectrique à contrainte constante (matrice 3×3) en $F.m^{-1}$

$[\epsilon^\varepsilon]$ = permittivité diélectrique à déformation constante (matrice 3×3) en $F.m^{-1}$

Constantes mécaniques :

$[s^E]$ = matrice de souplesse à champ électrique constant (matrice 6×6) en $m^2.N^{-1}$

$[s^D]$ = matrice de souplesse à déplacement électrique constant (matrice 3×3) en $m^2.N^{-1}$

$[c^E]$ = matrice de raideur à champ électrique constant (matrice 6×6) en $N.m^{-2}$

$[c^D]$ = matrice de raideur à déplacement électrique constant (matrice 3×3) en $N.m^{-2}$

Structures intelligentes

Fonction capteur sur une structure mince de type plaque :

$$V_Q(K, C_p, \mathcal{X}, \mathcal{Y}) = \frac{K}{C_p}\Big((\mathcal{X}_i'(x_2) - \mathcal{X}_i'(x_1)) \int_{y_1}^{y_2} \mathcal{Y}_{q_i}(y)dy + (\mathcal{Y}_i'(y_2) - \mathcal{Y}_i'(y_1)) \int_{x_1}^{x_2} \mathcal{X}_{p_i}(x)dx \Big)$$

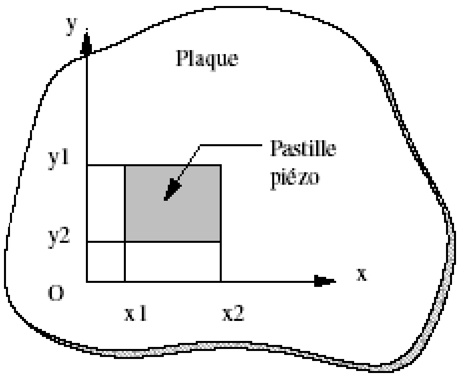

Fonction actionneur sur une structure mince de type plaque :

$$M_f(K, V_a, x, y) = K\, V_a \left[\mathcal{H}(x - x_1) - \mathcal{H}(x - x_2)\right] \left[\mathcal{H}(x - y_1) - \mathcal{H}(x - y_2)\right]$$

Références :

Thèses de Leleu (2002), Bruant (1998)

Tutorial de Moheimani dans IEEE CST (Dunant&al 2001, Moheimani 2003, …)

Structures intelligentes

Supports expérimentaux :

Poutre encastrée-libre (Problème d'Euler-Bernoulli)

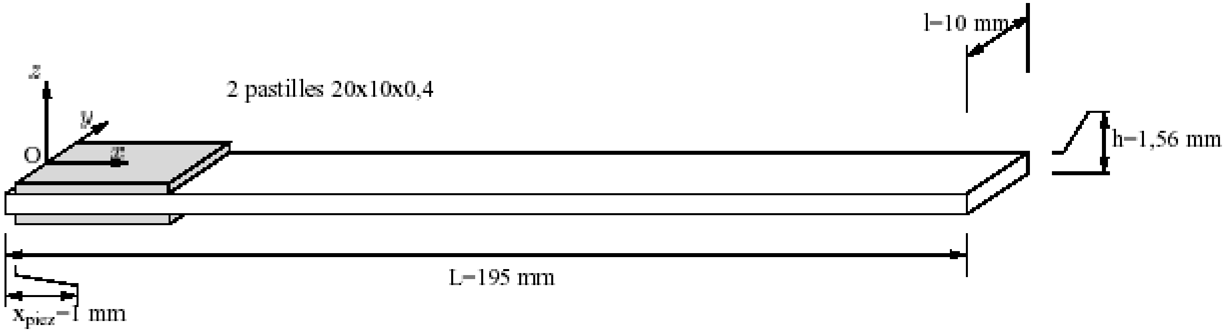

Un capteur, un actionneur **colocalisés**, placé à l'encastrement

Structures intelligentes

Supports expérimentaux :

Plaque simple :

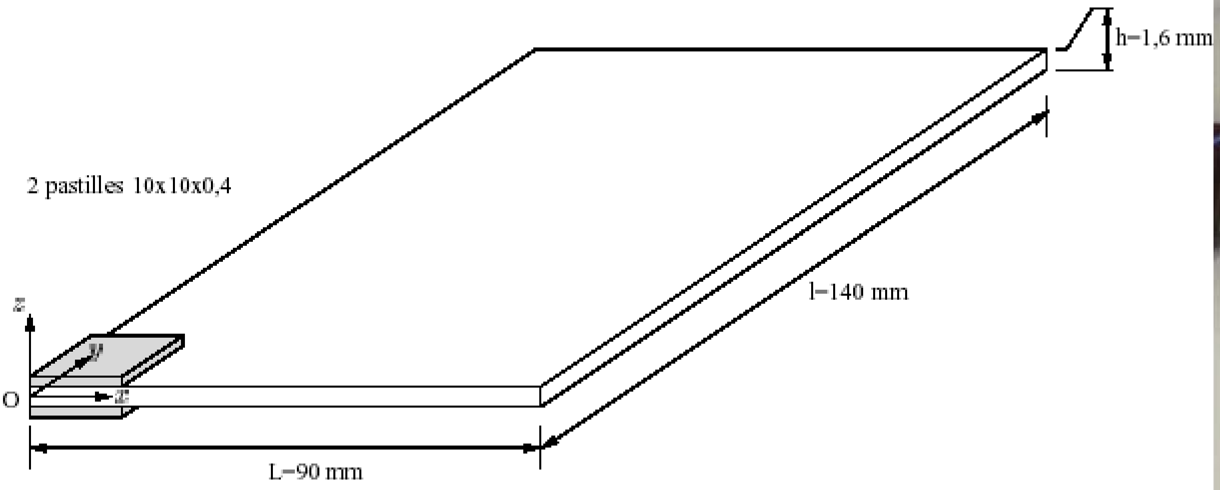

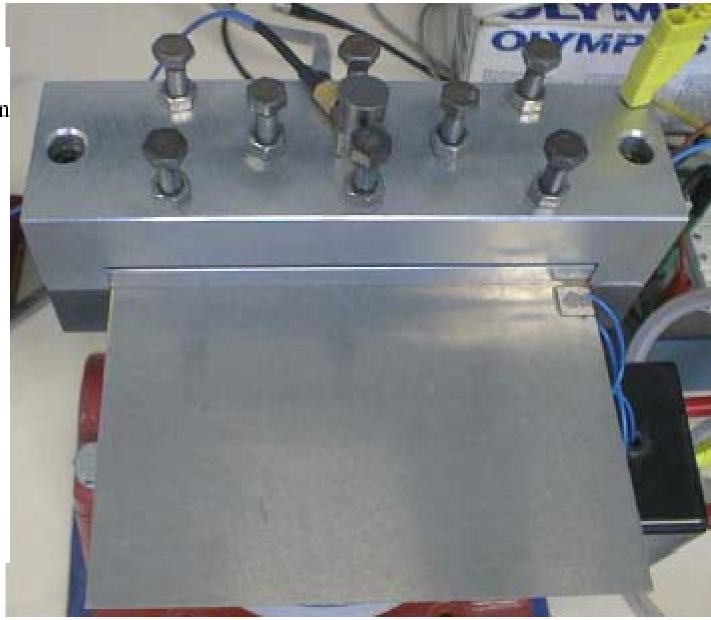

Un capteur, un actionneur **colocalisés**, placé dans un coin au niveau de l'encastrement

Structure excitée par pot vibrant

Structures intelligentes

Supports expérimentaux :

Structure de type plaque :

5 capteurs, **2** actionneurs placés sur une face de la structure

Structure excitée par pot vibrant

Développée conjointement LMT/SATIE

(Thèse de F. Formosa, 2002)

Placement des transducteurs

- Minimisation de l'énergie de commande

$$J = \int_0^{T_f} u^2(t)dt$$

On montre que la valeur minimum de l'énergie est

$$J = x(0^+)^T W_c^{-1}(T_f)x(0^+) \quad \text{avec} \quad W_c(T_f) = \int_0^{T_f} e^{A\tau}BB^Te^{A^T\tau}\mathrm{d}\tau$$

GRAMIEN DE COMMANDABILITE

⇒ Maximiser une norme du gramien de commandabilité

- Maximisation d'un critère dépendant de l'énergie transmise par l'actionneur à la structure

$$J_{\mathcal{E}} = \int_0^{\infty} \mathcal{E}(t)\mathrm{d}t$$

On montre que

$$\begin{aligned} J_{\mathcal{E}} &= \frac{1}{2}\mathrm{trace}\ (\int_0^{\infty} e^{At}BB^Te^{A^Tt})\mathrm{d}t \\ &= \frac{1}{2}\mathrm{trace}\ W_c \end{aligned}$$

⇒ Maximiser la trace du gramien de commandabilité

Placement des transducteurs

- Interprétation géométrique du gramien de commandabilité : **l’ellipsoïde de commandabilité**

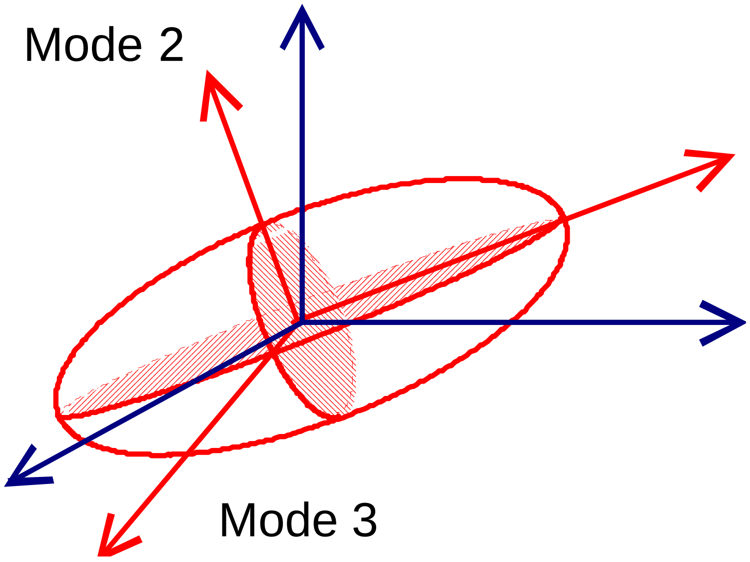

- Remarque : équivalence des divers critères énergétiques
- Degré de commandabilité :

$$\mathbf{trace}\ (W_c)\ \sqrt[2N]{(\mathbf{det}\ W_c)}/\sigma(\lambda_i)$$

Placement des transducteurs

Application à la plaque simple encastrée-libre

Placement optimal actionneur

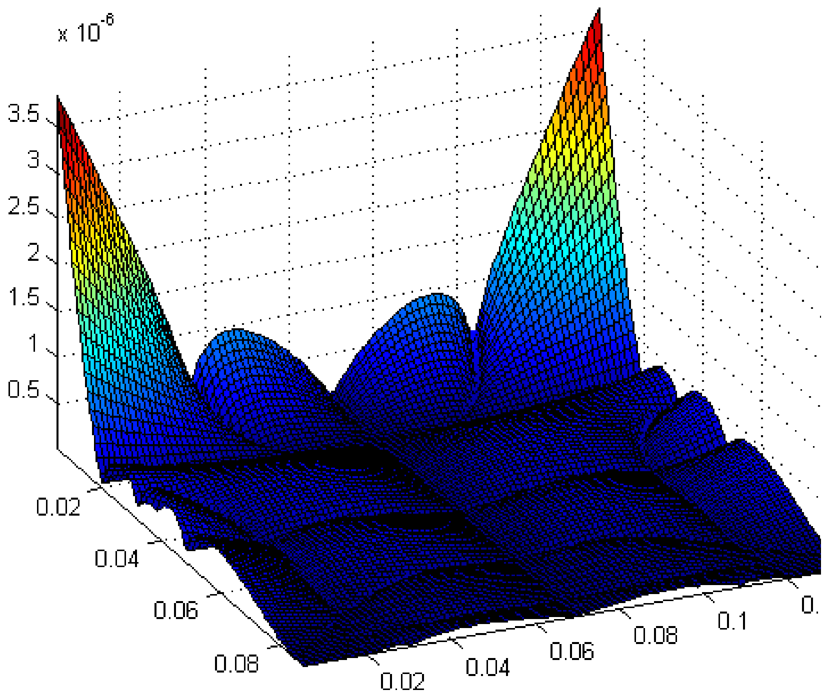

Placement optimal capteur

$$J_c = \int_0^\infty y^2 \mathrm{d}t$$

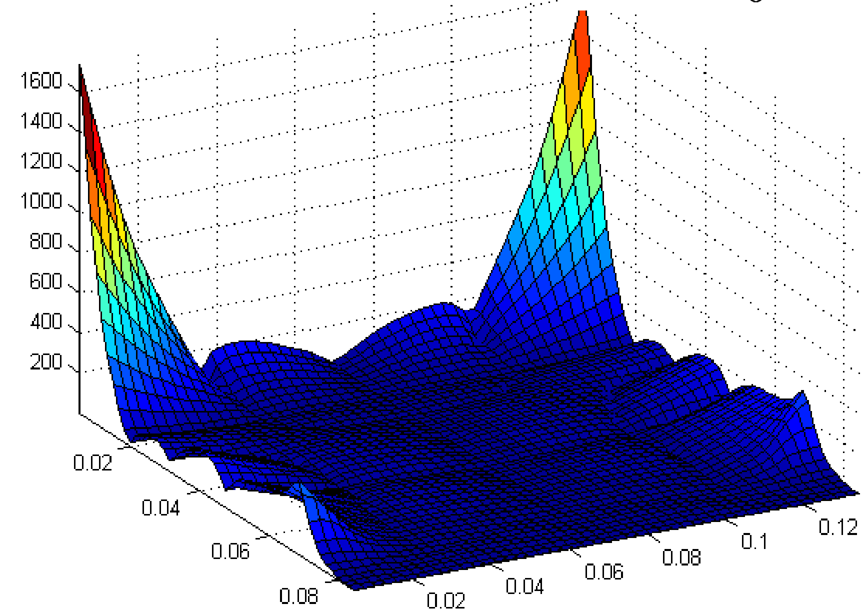

Dualité $\Rightarrow$ Colocalisation du capteur et de l'actionneur

Placement des transducteurs

Amélioration des méthodes de placement

- **Prise en compte de la perturbation**

1. Calcul du gramien de commandabilité perturbation-capteur pour déterminer les modes les plus excités
2. Synthèse d’un degré de commandabilité et d’un degré d’observabilité pondéré par l’efficacité recherchée sur chacun des modes à contrôler
3. Critère purement mécanique (déformation de Von Misès, …)

Dimensionnement des pastilles

Cas de l'actionneur piézoélectrique sur une poutre encastrée-libre :

- Maximiser le moment transmis par l'actionneur en la variable d'épaisseur

$$m_x = \frac{\beta(\zeta+1)}{1+\beta(6\zeta+12\zeta^2+8\zeta^3)}\, d_{31}\, l\, h\, Y_1\, V_a$$

où $\beta = Y_{1_p}/Y_1$ **matériaux**

$\zeta = t_p/h$ **épaisseur**

sous les contraintes :

$$\begin{cases} E = \dfrac{V_a}{t_p} \leq E_{max} \\ V_a \leq V_{a_{max}} = 500V \end{cases}$$

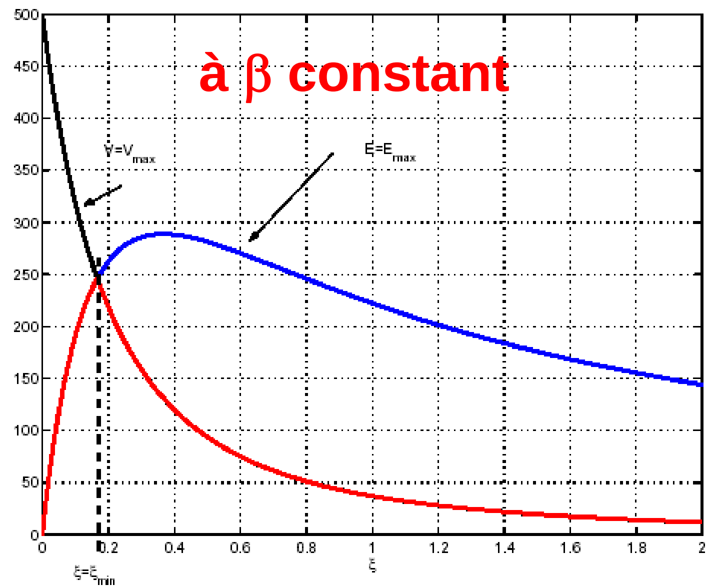

Extension au cas 2D : plaque

Cf. Thèse TLIBA, 2004

Dimensions hors-épaisseur :

Cf M. Collet, IEEE CST 2000

Dimensionnement des pastilles

Cas du capteur piézoélectrique sur une poutre encastrée-libre :

- Maximiser la tension électrique aux bornes du capteur en la variable d'épaisseur

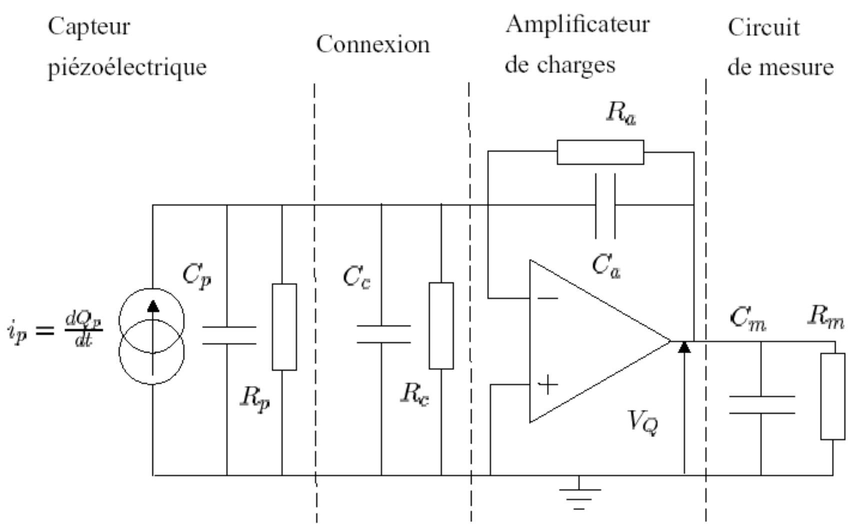

$$V_{c_Q}(t) = \frac{K_c}{C_a}\int_{S_p}\left(\frac{\partial^2 w}{\partial x^2} + \frac{\partial^2 w}{\partial y^2}\right)dS$$

$$K_c = e_{31}\left(\frac{h}{2} + \frac{t_p}{2}\right)$$

$$K_c = e_{31}\left(\frac{h}{2} + t_p\right)$$

$$\frac{V_{c_Q}}{V_{c_T}} = \frac{C_p}{C_a}$$

⇒ Tension proportionnelle à l'épaisseur

Stratégie d'étude

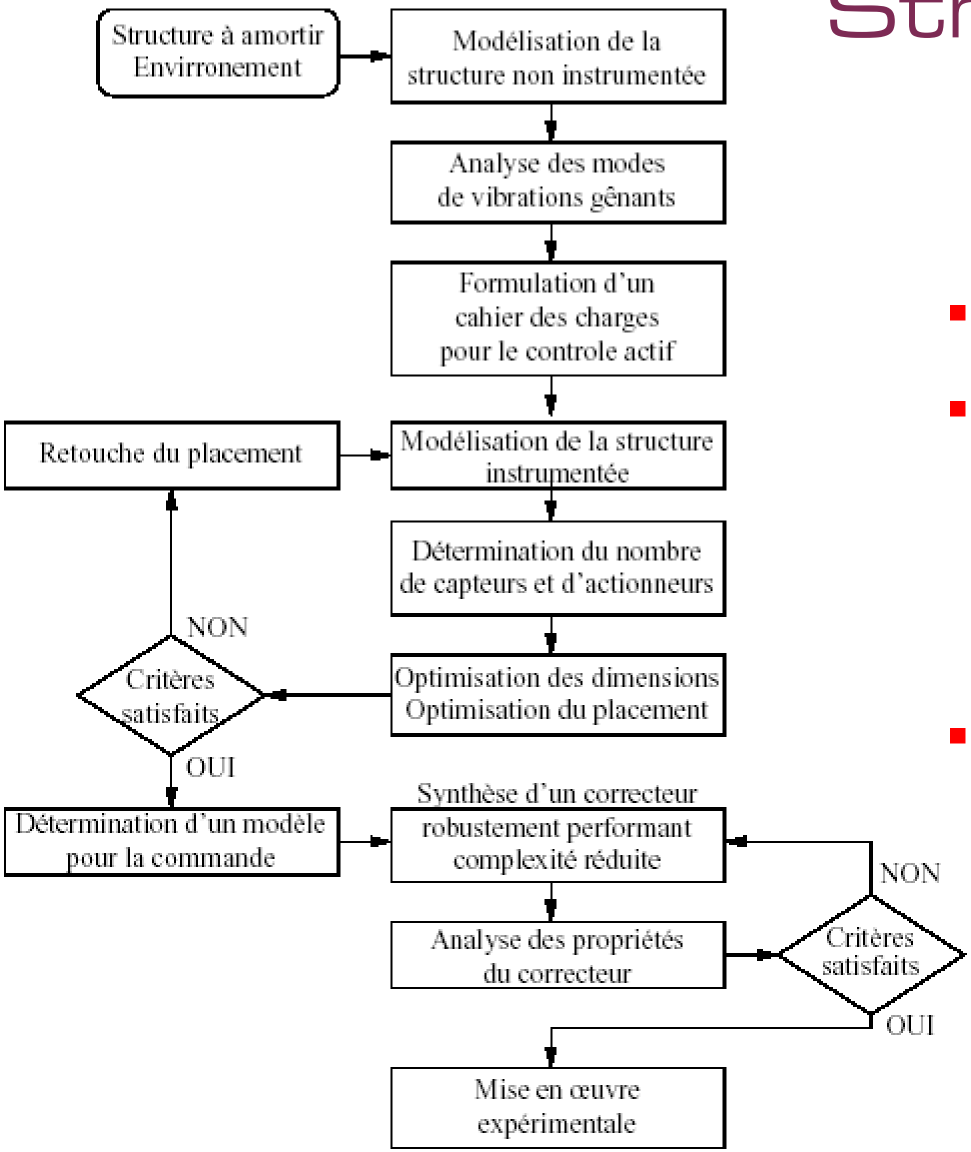

- Prototypage virtuel
- Démarche itérative alternant
  - Modélisation
  - Placement
  - Commande
- Finalité expérimentale

Modélisation d'une structure intelligente

Une approche de résolution par la méthode des éléments finis

Formulation du problème EDP

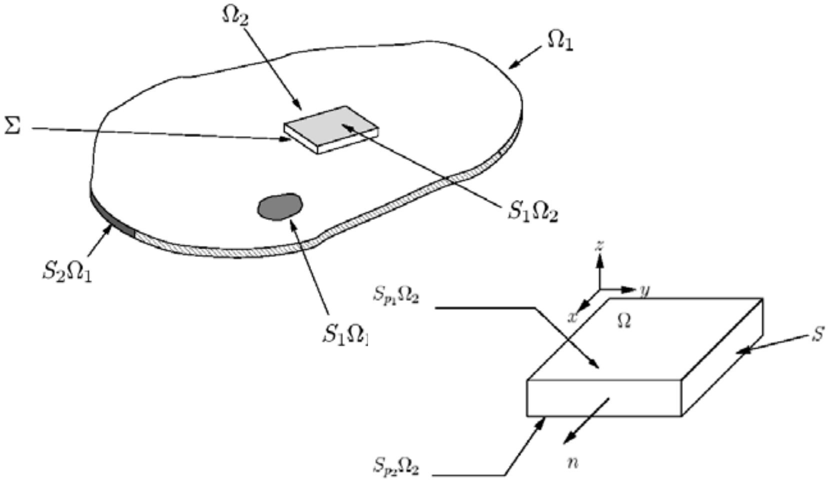

Un problème ***multiphysique***

- Comportement mécanique de la structure mince
- Comportement électromécanique du composant actif
- Problème de modélisation de l'**intéraction électromécanique pastille/structure**

Équations d'équilibre et relations de comportement

mécanique

$$\sigma_{ij,j} + f_i = \rho \ddot{u}_i$$

$$\text{avec } \sigma_{ij} = \sigma_{ji}$$

$$\varepsilon_{ij} = \frac{1}{2}(u_{i,j} + u_{j,i})$$

$$\sigma_{ij} = C_{ijkl}\varepsilon_{kl}$$

électrique

$$D_{i,i} = q$$

$$= 0$$

$$E_i = -\phi_{,i}$$

$$\sigma = c\,\varepsilon - e^T E$$

$$D = e\,\varepsilon + \epsilon\, E$$

Conditions aux limites type Neumann et Dirichlet

$$u = U_d \quad \text{sur} \quad S_u$$

$$\sigma\, n = F_\sigma \quad \text{sur} \quad S_\sigma$$

$$\phi = \Phi_0 \quad \text{sur} \quad S_\phi$$

$$D\, n = Q_d \quad \text{sur} \quad S_q$$

$$D\, n = 0 \quad \text{sur } S_{p1}\Omega_2$$

$$\phi = 0 \quad \text{sur } S_{p2}\Omega_2$$

$$\phi = \Phi_0(t) \text{ sur } S_{p1}\Omega_2$$

Conditions initiales

$$u(t=0) = 0$$

$$\dot{u}(t=0) = 0$$

$$\Phi_0(t=0) = 0$$

Formulation variationnelle

Champ de déplacement virtuel généralisé

$$\delta w = \begin{bmatrix} \delta u \\ \delta \phi \end{bmatrix}$$

Principe de Hamilton (conservatif) :

$$\delta \left(\int_{t_1}^{t_2} (T - V)\, dt \right) = 0$$

Energie cinétique : $T = \frac{1}{2} \int_{\Omega} \rho \dot{u}_i \dot{u}_i \, d\Omega$

Energie potentielle étendue : $V \;=\; H - W$

Energie électromécanique : $H = \frac{1}{2} \int_{\Omega_1} \sigma_{ij} \varepsilon_{ij} \, d\Omega_1 + \frac{1}{2} \int_{\Omega_2} \sigma_{ij} \varepsilon_{ij} \, d\Omega_2 - \int_{\Omega_2} D_i E_i \, d\Omega_2$

Travail des forces extérieures : $W = \int_S F_{\sigma_i} u_i \, dS - \int_S Q_d \phi \, dS + \int_{\Omega} f_i u_i \, d\Omega - \int_{\Omega} q \phi d\Omega$

Formulation éléments finis

Cas du composant piézoélectrique seul :

- Formulation de l'élément **Hexa8** à 4 ddls par nœud (3 translations, 1 potentiel électrique)
- Hypothèse : champs linéaires dans l'élément (fonction d'interpolation de degre 1)

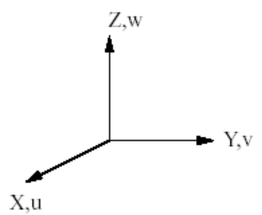

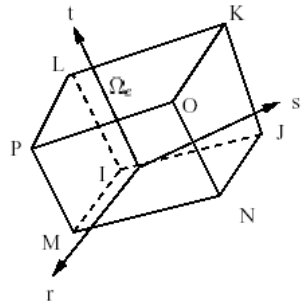

$$\begin{bmatrix} M^e & 0 \\ 0 & 0 \end{bmatrix} \begin{pmatrix} \ddot{u} \\ \ddot{\phi} \end{pmatrix} + \begin{bmatrix} K^e_{uu} & K^e_{u\phi} \\ {K^e_{u\phi}}^T & K^e_{\phi\phi} \end{bmatrix} \begin{pmatrix} u \\ \phi \end{pmatrix} = \begin{pmatrix} F^e_u \\ F^e_Q \end{pmatrix}$$

$$u^e = \frac{1}{8}\big(u_I(1-s)(1-t)(1-r) + u_J(1+s)(1-t)(1-r) \\ + u_K(1+s)(1+t)(1-r) + u_L(1-s)(1+t)(1-r) \\ + u_M(1-s)(1-t)(1+r) + u_N(1+s)(1-t)(1-r) \\ + u_O(1+s)(1+t)(1+r) + u_P(1-s)(1+t)(1+r)\big)$$

$$\phi^e = \frac{1}{8}\big(\phi_I(1-s)(1-t)(1-r) + \phi_J(1+s)(1-t)(1-r) \\ + \phi_K(1+s)(1+t)(1-r) + \phi_L(1-s)(1+t)(1-r) \\ + \phi_M(1-s)(1-t)(1+r) + \phi_N(1+s)(1-t)(1-r) \\ + \phi_O(1+s)(1+t)(1+r) + \phi_P(1-s)(1+t)(1+r)\big)$$

$$M^e = \int_{\Omega_e} \rho\, N_u\, N_u^T\, d\Omega_e$$

$$K^e_{uu} = \int_{\Omega_e} B_u\, c\, B_u^T\, d\Omega_e$$

$$K^e_{\phi\phi} = -\int_{\Omega_e} B_\phi^T\, \varepsilon\, B_\phi\, d\Omega_e$$

$$K^e_{u\phi} = \int_{\Omega_e} B_u^T\, e\, B_\phi\, d\Omega_e$$

$$F^e_u = \int_{\Omega_e} N_u^T\, f\, d\Omega_e + \int_{S_\sigma} N_u^T\, F_\sigma\, dS_\sigma$$

$$F^e_Q = -\int_{S_q} N_\phi^T\, \sigma\, dS_q$$

Formulation éléments finis

Choix du type d'élément pour modéliser la plaque : problème de l'intéraction

- **HEXA8** à 3 ddls par nœud sous le composant piézoélectrique
- **QUAD4** (élément plaque ou coque) à 6 ddls par nœud (3 translations + 3 rotations) (Cf. Batoz)
- $\Rightarrow$ Maillage en présence d'éléments de **topologie différente**

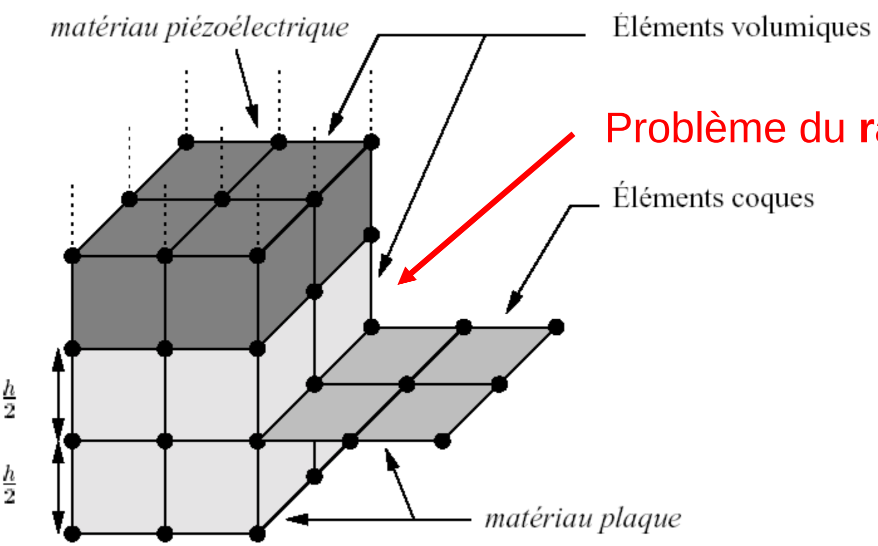

Problème du **raccordement** des éléments

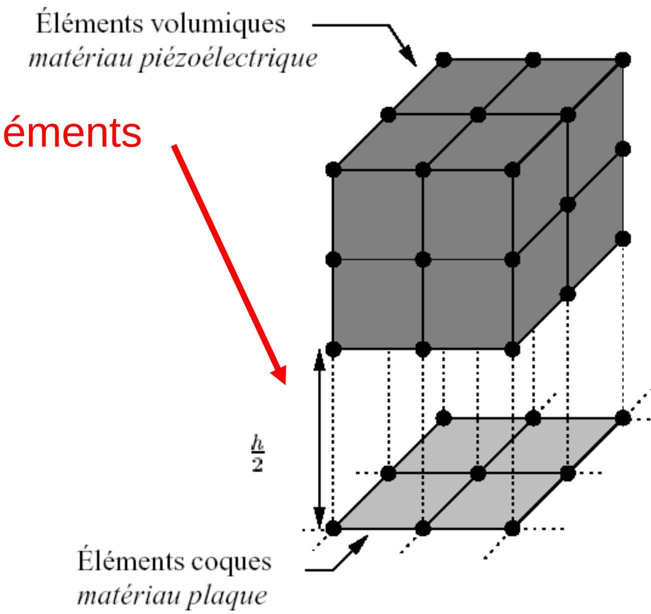

Formulation éléments finis

Raccordement « rigide » des éléments

⇒ *Hypothèses de Kirchoff-Love* :

1. La plaque est mince d'épaisseur h et possède un plan moyen. Les faces extérieures de la plaques sont les plans définis par $z = \pm\frac{h}{2}$
2. Seul le déplacement transversal $w(x, y, z, t)$ est considéré.
3. La contrainte σ_z dans la direction transversale est nulle en tout point de l'épaisseur.
4. L'épaisseur reste constante.
5. Une perpendiculaire à la surface moyenne reste perpendiculaire au cours du mouvement. La déformation en cisaillement transverse est donc négligée.
6. Les déplacements u et v dans le plan Oxy résultent de deux effets distincts :
   – un champ de déplacement initial et uniforme selon l'épaisseur, correspondant à une déformation du type traction-compression (ou membranaire),
   – le champ de déplacement dû à la rotation de la section droite autour des axes U et V.

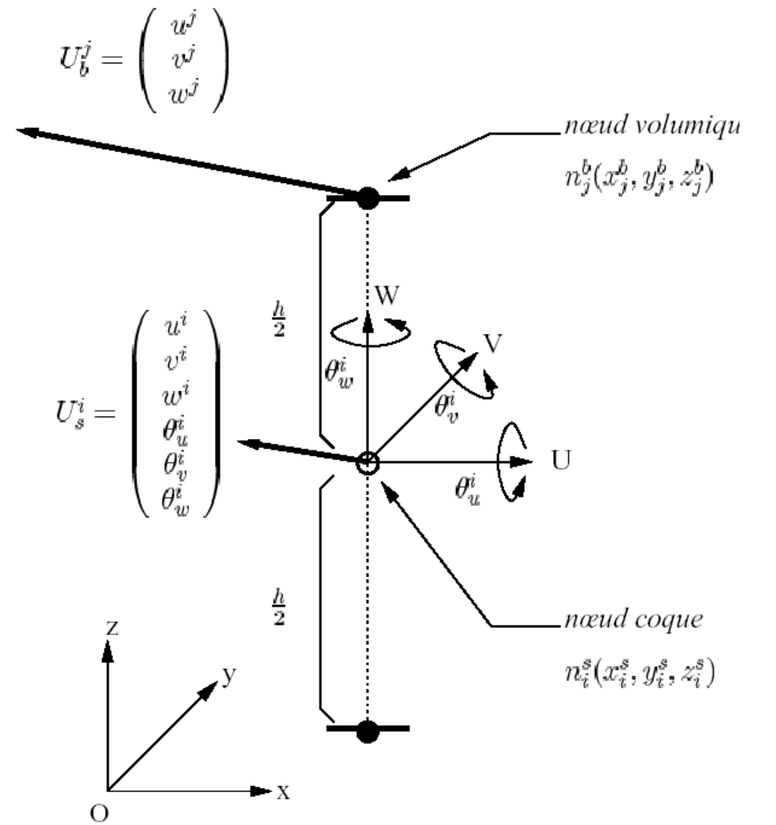

$$\begin{pmatrix} u^j \\ v^j \\ w^j \end{pmatrix} = \begin{pmatrix} u^i + z\,\theta_v^i \\ v^i - z\,\theta_u^i \\ w^i \end{pmatrix}$$

Formulation éléments finis

Equations de mouvement et d'observation de la structure instrumentée d'un capteur et d'un actionneur :

$$\left\{ \begin{array}{rcl} M\,\ddot{u} + (K_{uu} + {K^c_{u\phi}}^T (K^c_{\phi\phi})^{-1} K^c_{u\phi})\,u & = & F_u - {K^a_{u\phi}}^T \Phi^a \\ \phi^c & = & (K^c_{\phi\phi})^{-1} K^c_{u\phi}\,u \end{array} \right.$$

Système différentiel du 2nd ordre à coef. Constants

!!! Ordre élevé en général (~1000 à 100 000)

Algorithme de mise à jour des matrices de masse, de raideur et des forces généralisées

$$\begin{array}{rcl} K^*_{kj} & = & K_{kj} - C^*_j\,K_{ki} - C^*_k\,K_{ij} + C^*_k C^*_j K_{ii} \\ M^*_{kj} & = & M_{kj} - C^*_j\,M_{ki} - C^*_k\,M_{ij} + C^*_k C^*_j M_{ii} \\ F^*_k & = & F_k - C^*_0\,K_{ki} - C^*_k F_i + C^*_k C^*_0 K_{ii} \end{array}$$

Applications

Cas de la poutre : comparaison des 2 approches

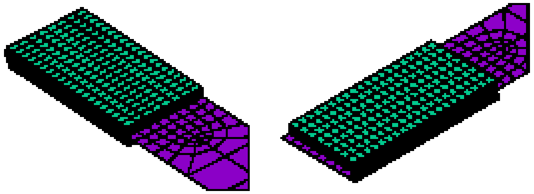

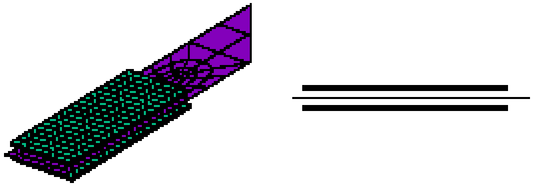

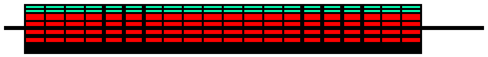

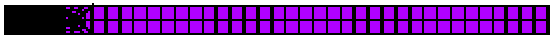

Matériau	**Type d'élément**	**Nb. d'éléments**	**Nb. total de nœuds**
piézoélectrique	volumique	640	1134
poutre AU4G	coque	264	327
TOTAL		**904**	**1461**

Applications

Cas de la plaque simple : influence du maillage

Choix de la méthode QUAD4 pure pour la plaque et HEXA8 pour les pastilles,

2 paramètres d’influences sur les fréquences propres et le gain statique :

- Discrétisation de l’épaisseur
- Dimensions hors-épaisseur

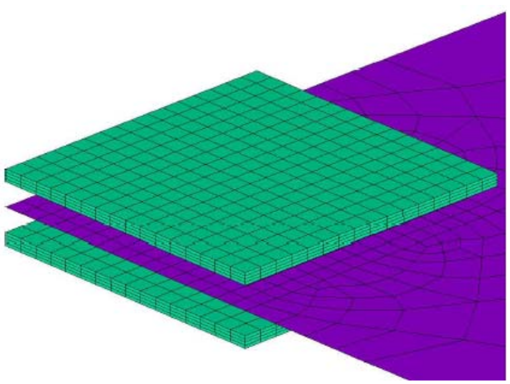

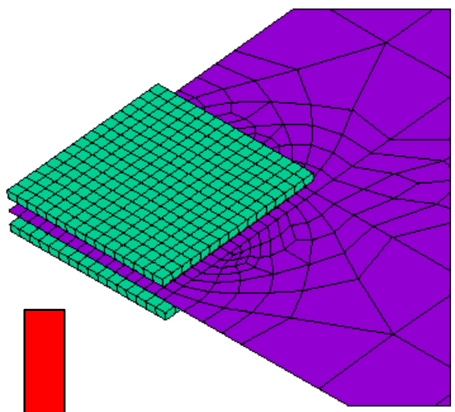

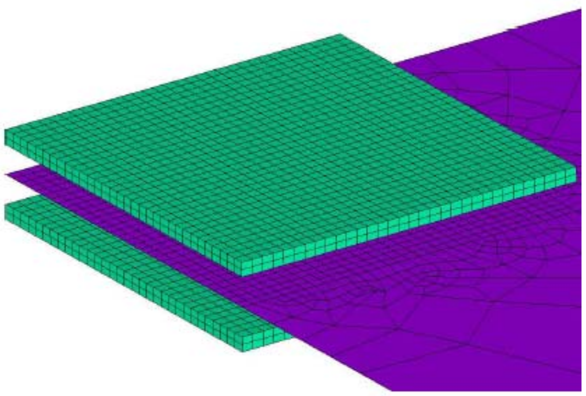

Meilleur compromis temps de calcul/qualité des résultats

Applications

Cas de la plaque simple : influence du maillage

Convergence des fréquences propres

	8x8x1	16x16x1	4x4x2	8x8x2	16x16x2	32x32x4	**Variation (en %)**
mode 1	165,43	165,42	165,41	165,40	165,40	165,39	**0.02**
mode 2	299,37	299,35	299,30	299,27	299,27	299,25	**0.04**
mode 3	655,57	655,55	655,47	655,44	655,44	655,25	**0.05**
mode 4	1036,5	1036,5	1036,4	1036,4	1036,4	1036,3	**0.02**
mode 6	1227,7	1227,5	1227,2	1227,2	1227,2	1227,1	**0.05**

Convergence du gain statique du transfert actionneur/capteur

	8x8x1	16x16x1	4x4x2	8x8x2	16x16x2	32x32x4	**Variation (en %)**
Gain stat.	-0.040357	-0.040357	-0.040357	-0.040357	-0.040357	-0.040356	$\simeq$**0.0**

Applications

Cas de la structure de type plaque :

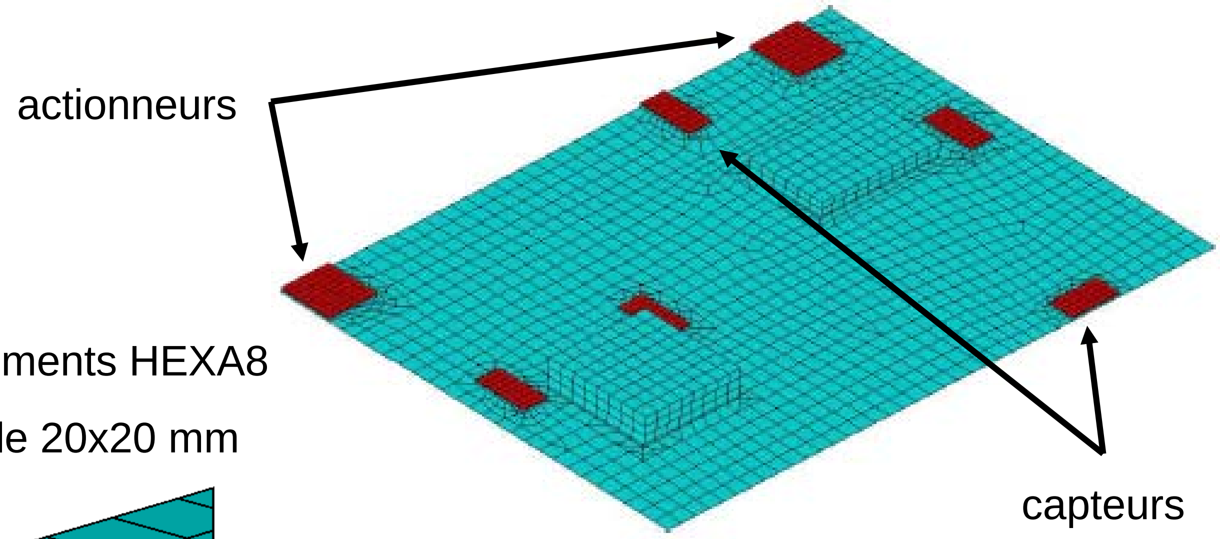

2 actionneurs

- Utilisation d'une couche d'éléments HEXA8
- 8x8 éléments pour une pastille 20x20 mm

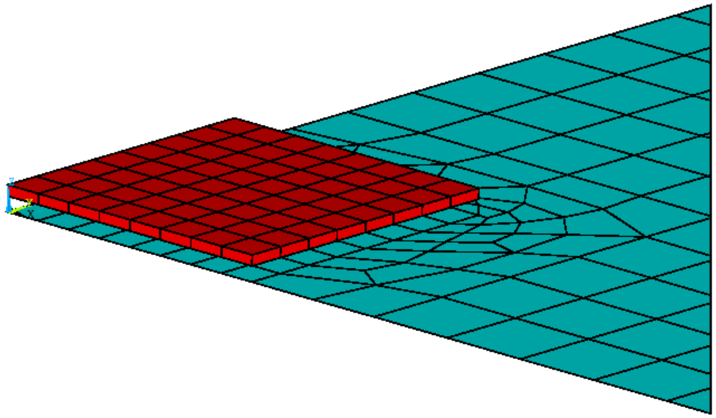

Modèle dynamique entrée(s)/sortie(s)

Besoin de réduction du modèle EF ⇒ projection dans la base modale réduite

$$u(x,y,z,t) = \boldsymbol{\eta}(x,y,z)\, q(t) \quad , \quad K\boldsymbol{\eta} = M\boldsymbol{\eta}\,\lambda \quad , \quad \boldsymbol{\eta}^T M \boldsymbol{\eta} = I_n \quad , \quad \lambda = diag\{\omega_i^2\}$$

$$\ddot{q}(t) + \Omega\, q(t) = 0 \qquad \boldsymbol{\eta}^T K \boldsymbol{\eta} = \Omega$$

Méthode de Lanczos : Calcul des r premiers modes $u(t) = \boldsymbol{\eta}_r(x,y,z)\, q_r(t)$ ⇒ **troncature**

⇒ Correction du gain statique nécessaire, ***mode(s) statique(s)*** pour ***enrichir la base modale réduite***

$$I_n\, \ddot{q}_r(t) + diag\{2\zeta_i\omega_i\}\dot{q}_r + diag\{\omega_i^2\}\, q_r(t) = \boldsymbol{\eta}_r^T F_u(t) + \boldsymbol{\eta}_r^T K_a \Phi_a(t)$$

$$\phi^c = K_c \boldsymbol{\eta}_r\, q_r(t)$$

Modèle dynamique entrée(s)/sortie(s)

Construction du modèle d'état :

$$\begin{cases} \dot{x}(t) = A\,x(t) + B_w\,w(t) + B\,u(t) \\ z(t) = F\,x(t) \\ y(t) = C\,x(t) \end{cases}$$

$$A = \begin{bmatrix} -C & -\Omega \\ I_n & 0 \end{bmatrix}$$

$$B = \begin{bmatrix} \boldsymbol{\eta}_r^T K_a \\ 0 \end{bmatrix}$$

$$B_w = \begin{bmatrix} \boldsymbol{\eta}_r^T M_{eq} \\ 0 \end{bmatrix}$$

$$C = \begin{bmatrix} K_c \boldsymbol{\eta}_r & 0 \end{bmatrix}$$

$$F = \begin{bmatrix} F_c \boldsymbol{\eta}_r & 0 \end{bmatrix}$$

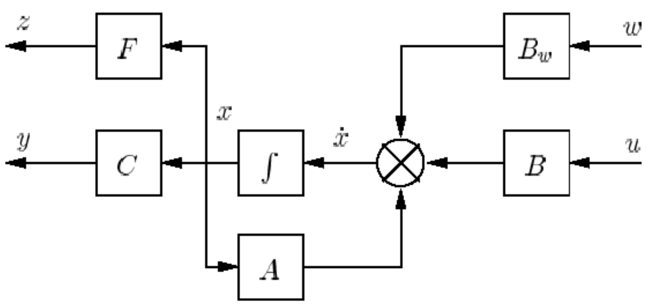

Applications

Cas de la poutre : réponse fréquentielle actionneur/capteur

Modes de flexion

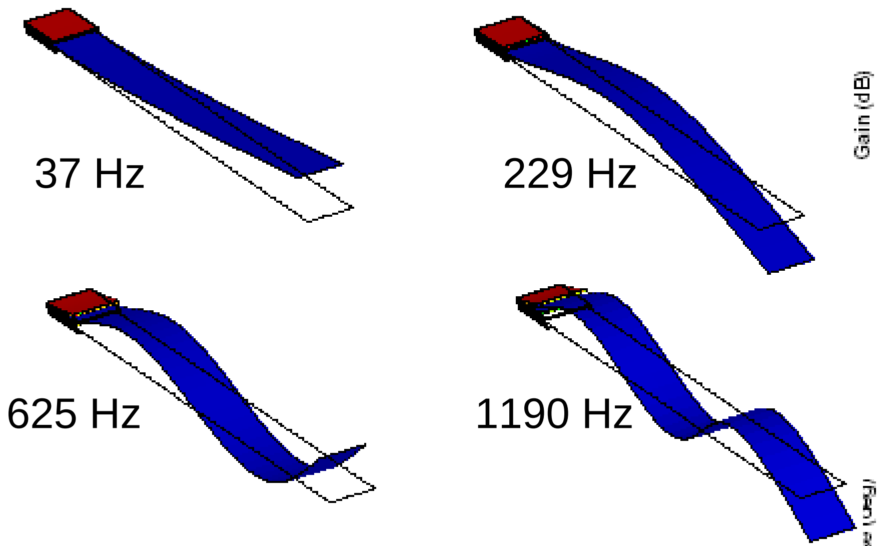

Modes statiques

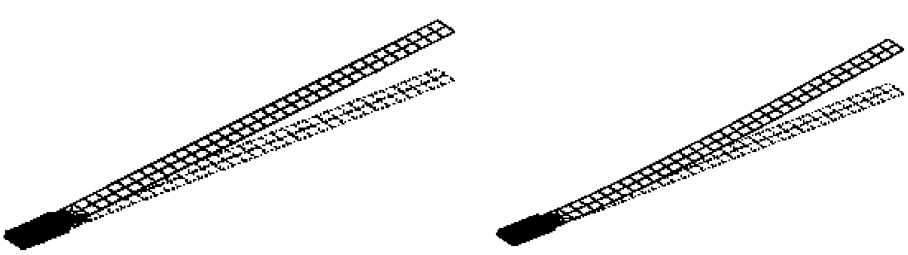

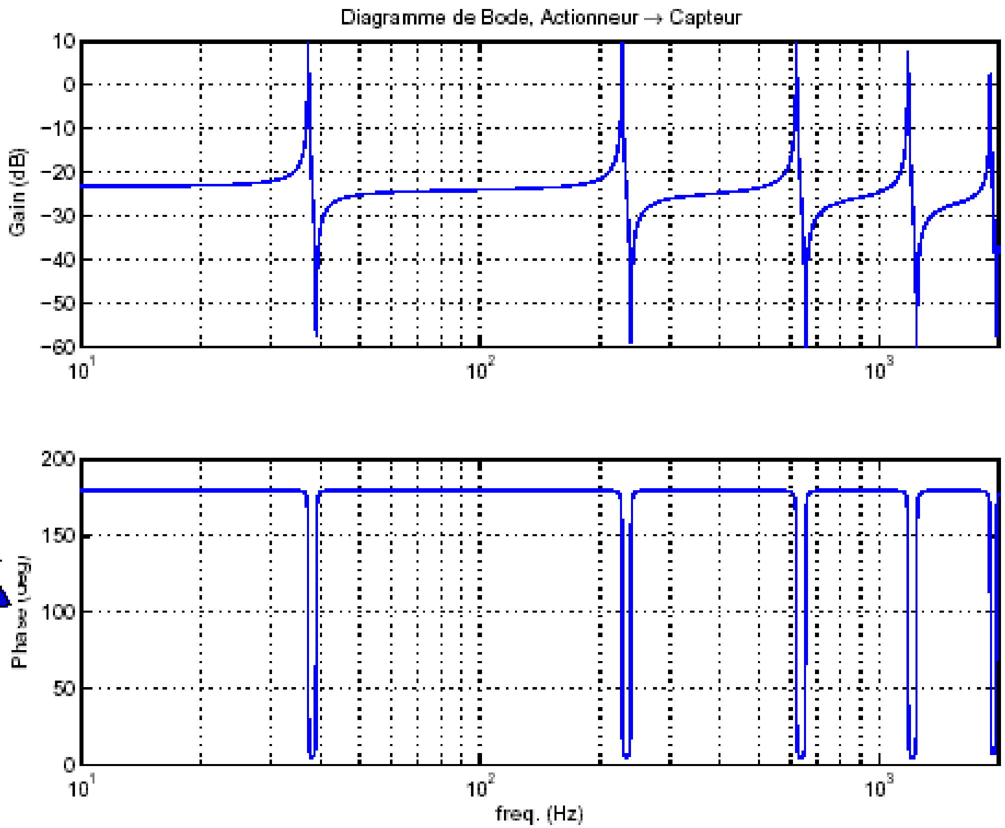

Applications

Cas de la plaque : réponse fréquentielle actionneur/capteur, pot/accéléro.

Modes

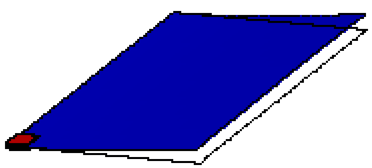

165 Hz

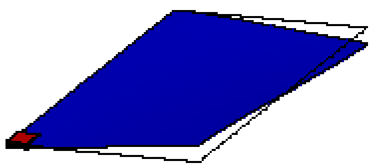

299 Hz

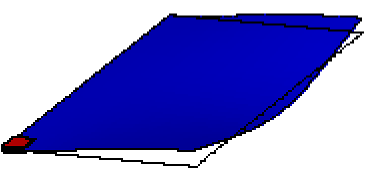

655 Hz

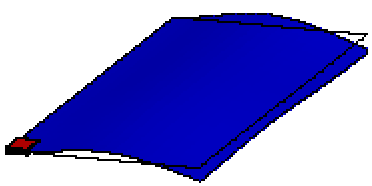

1036 Hz

Modes statiques

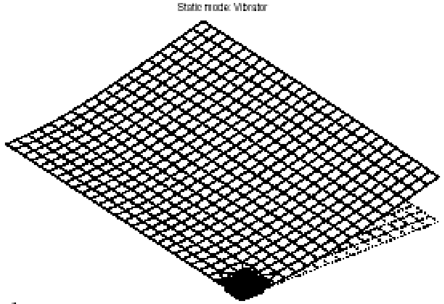

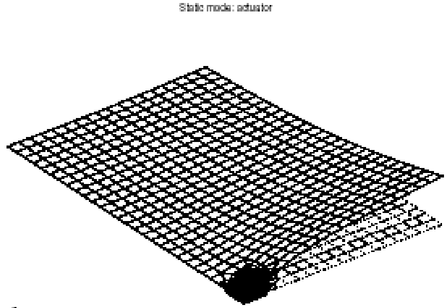

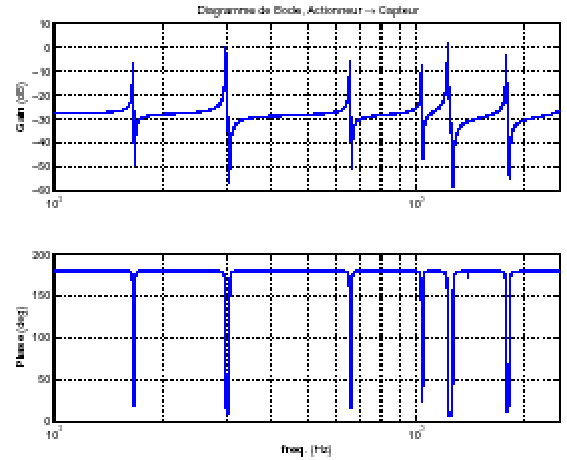

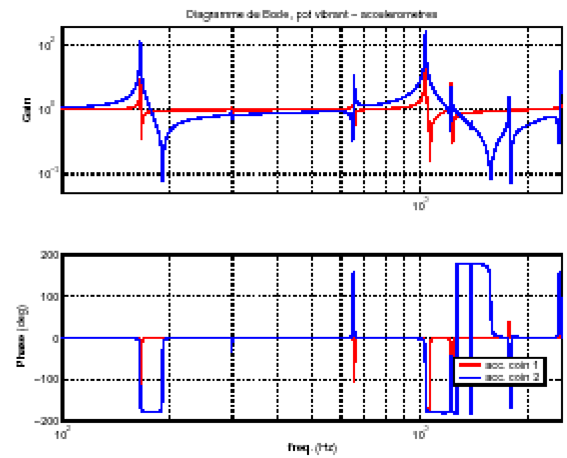

Applications

Cas de la plaque complexe : réponse fréquentielle actionneurs/capteurs,

Modes

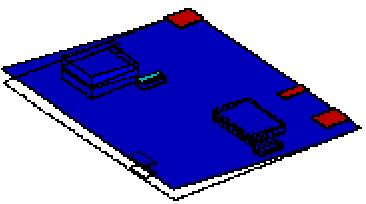

46 Hz

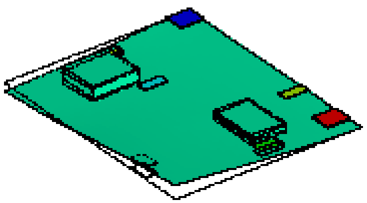

103 Hz

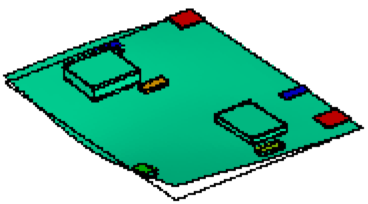

260 Hz

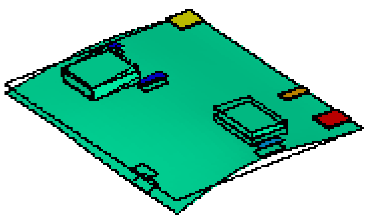

318 Hz

Mode statique, act1

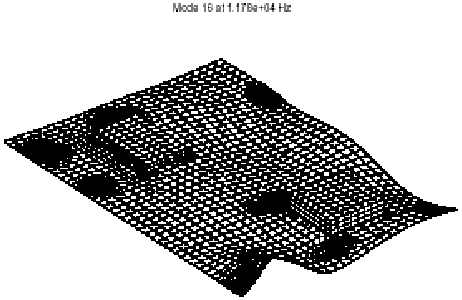

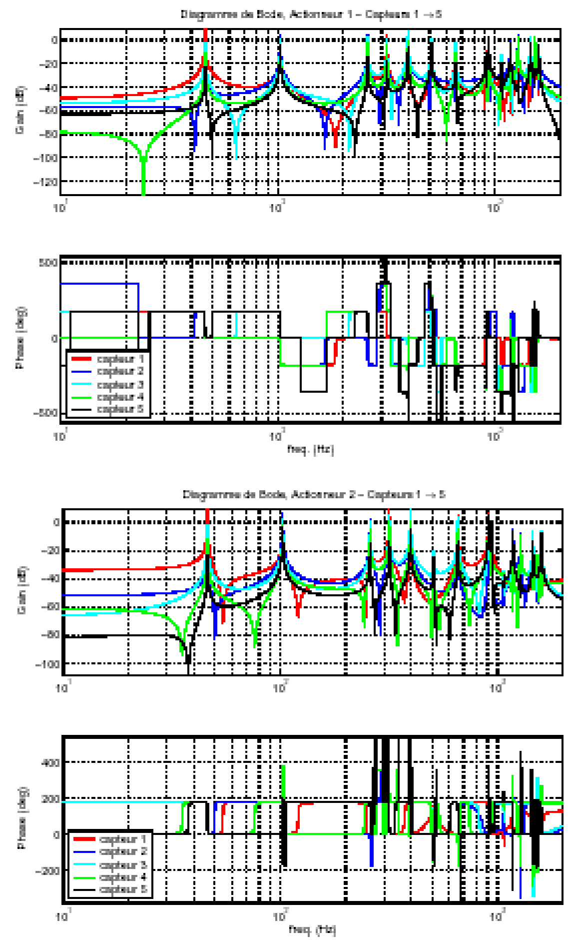

Mise en œuvre expérimentale

Dispositif expérimental

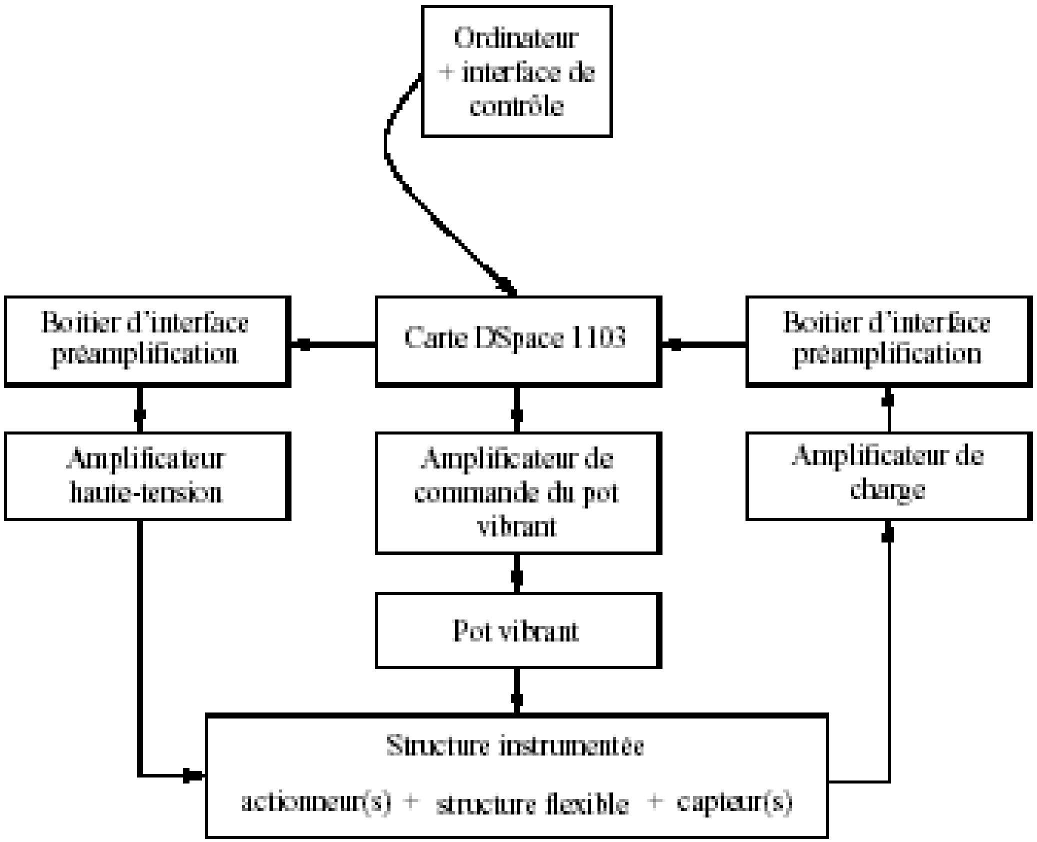

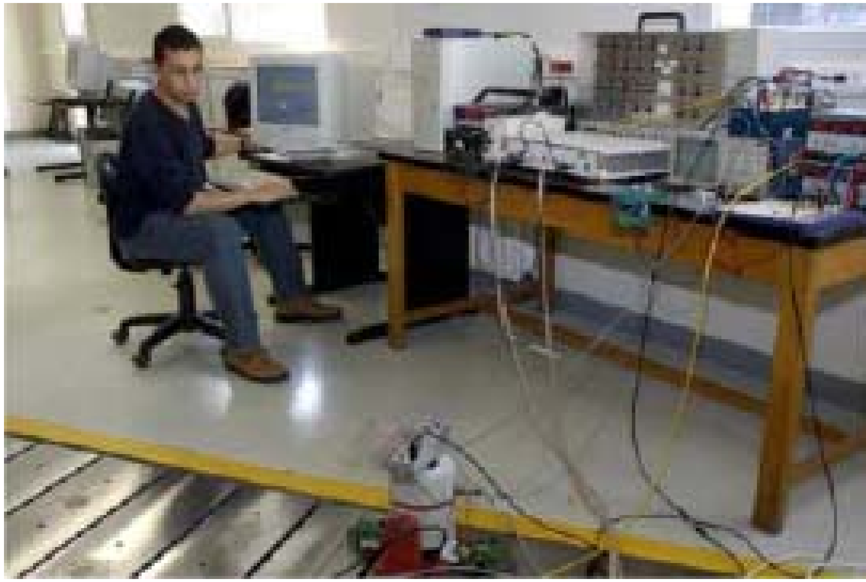

Dispositif expérimental

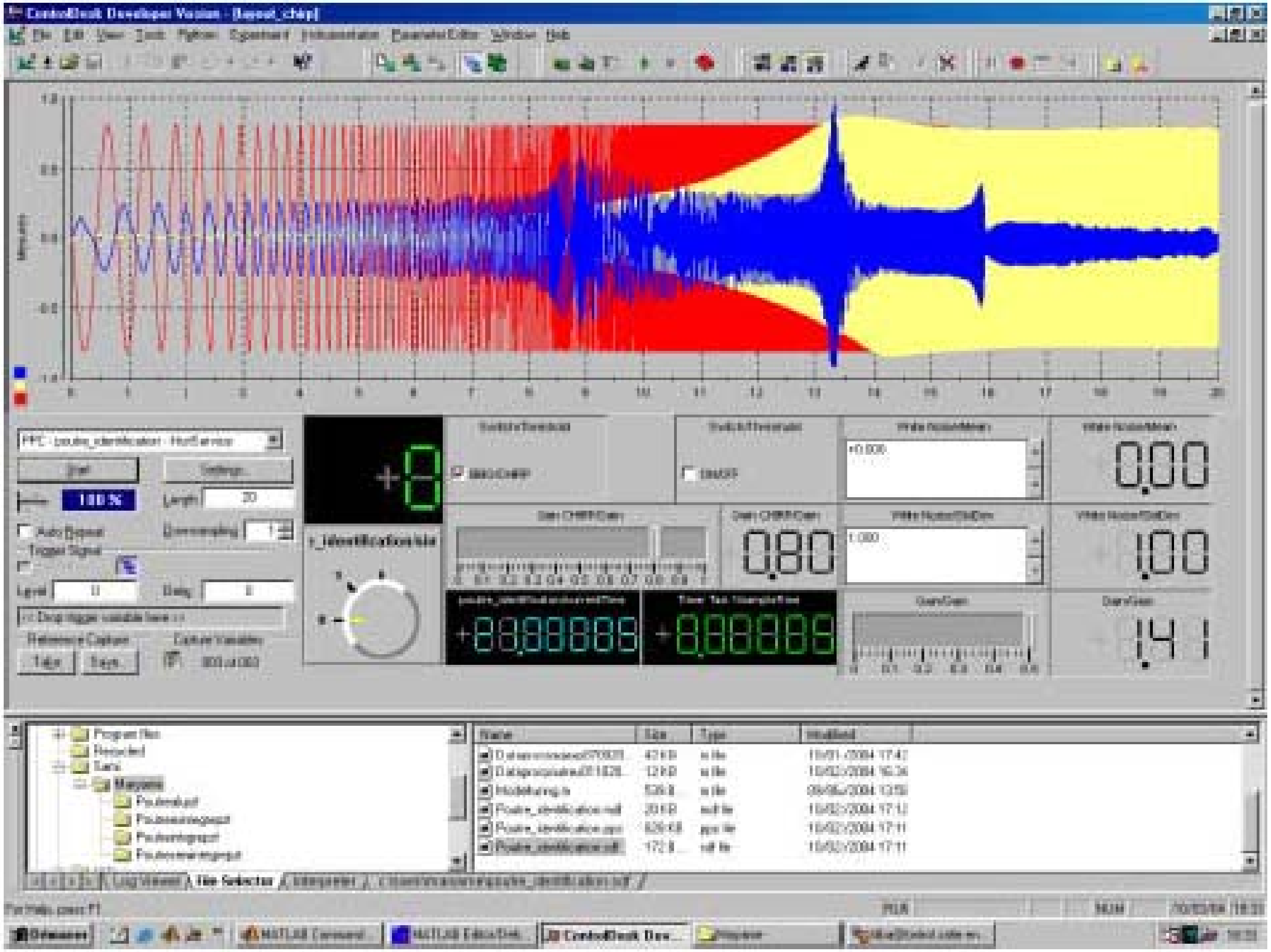

Comparaison simu./manip.

Cas de la poutre : réponse fréquentielle actionneur/capteur

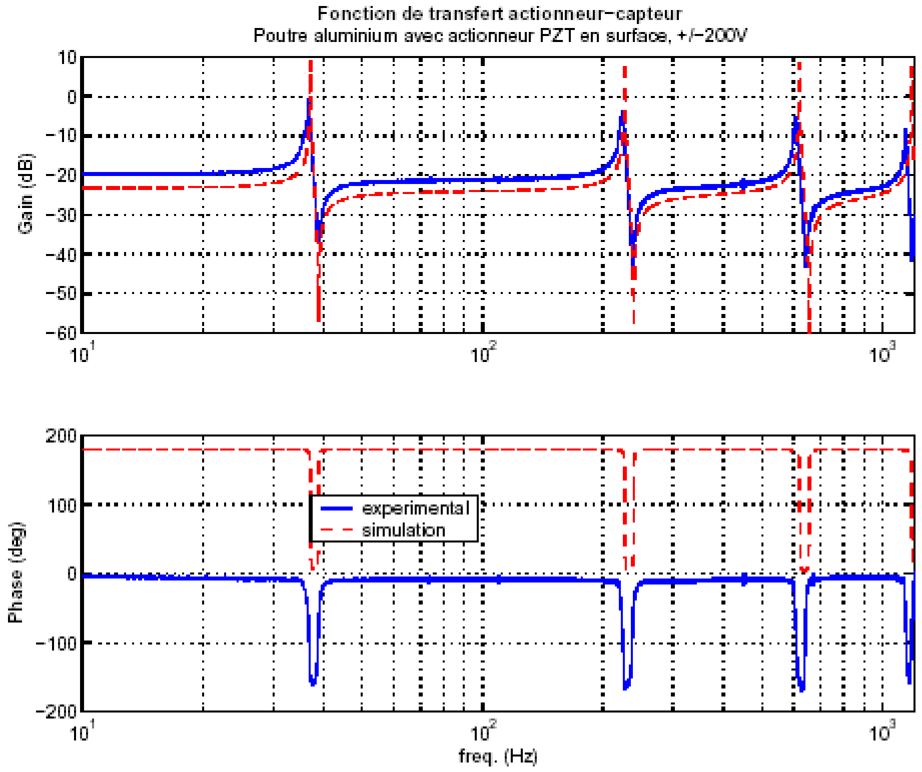

Comparaison simu./manip.

Cas de la plaque simple

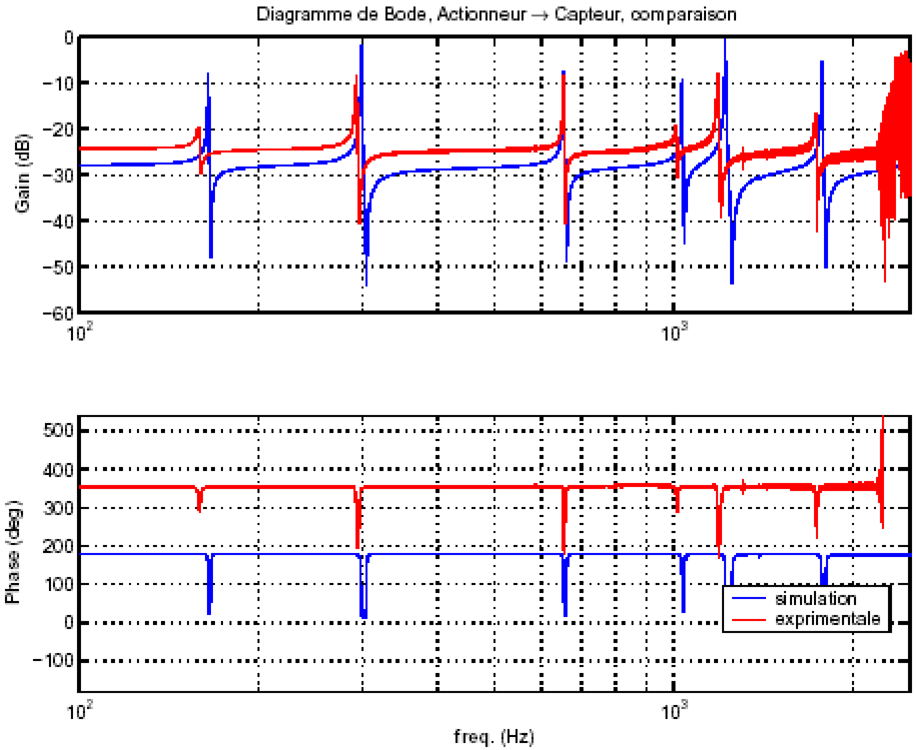

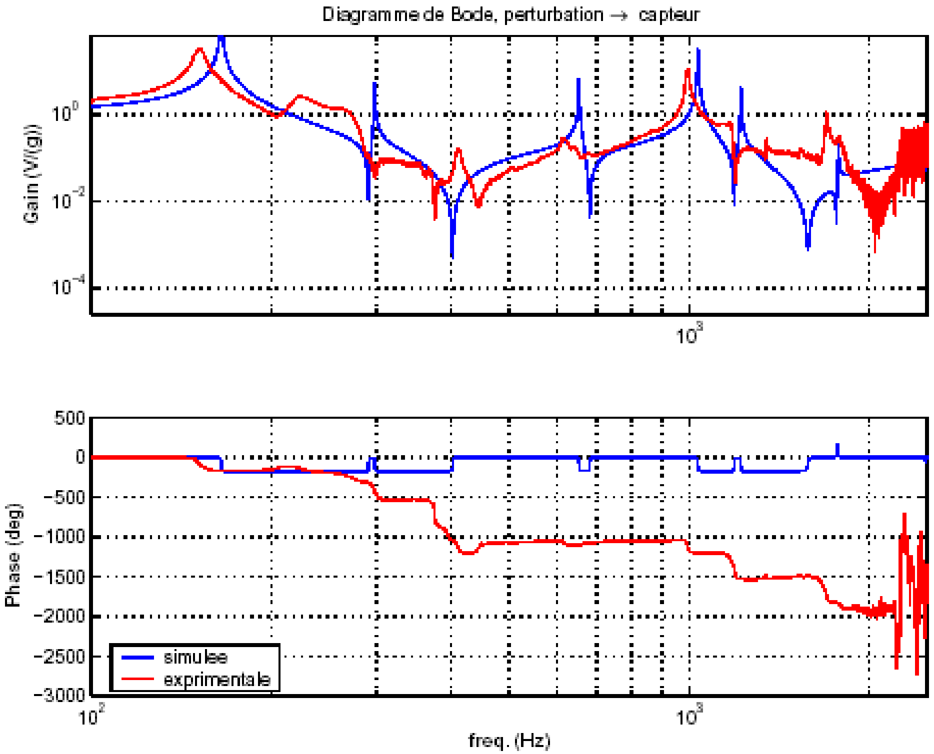

Comparaison simu./manip.

Cas de la plaque complexe

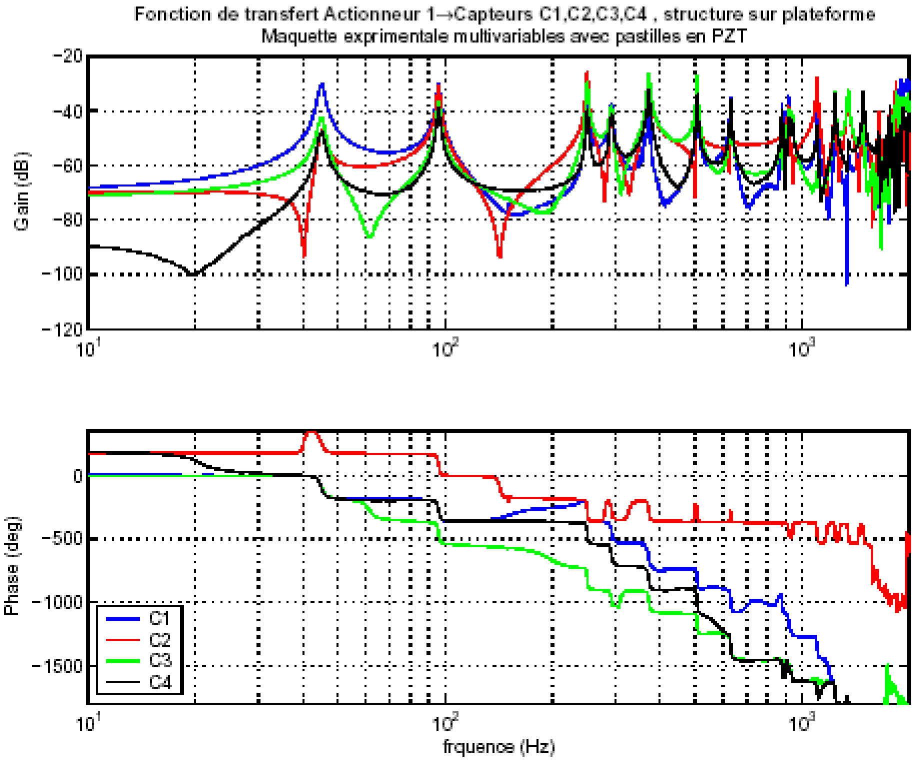

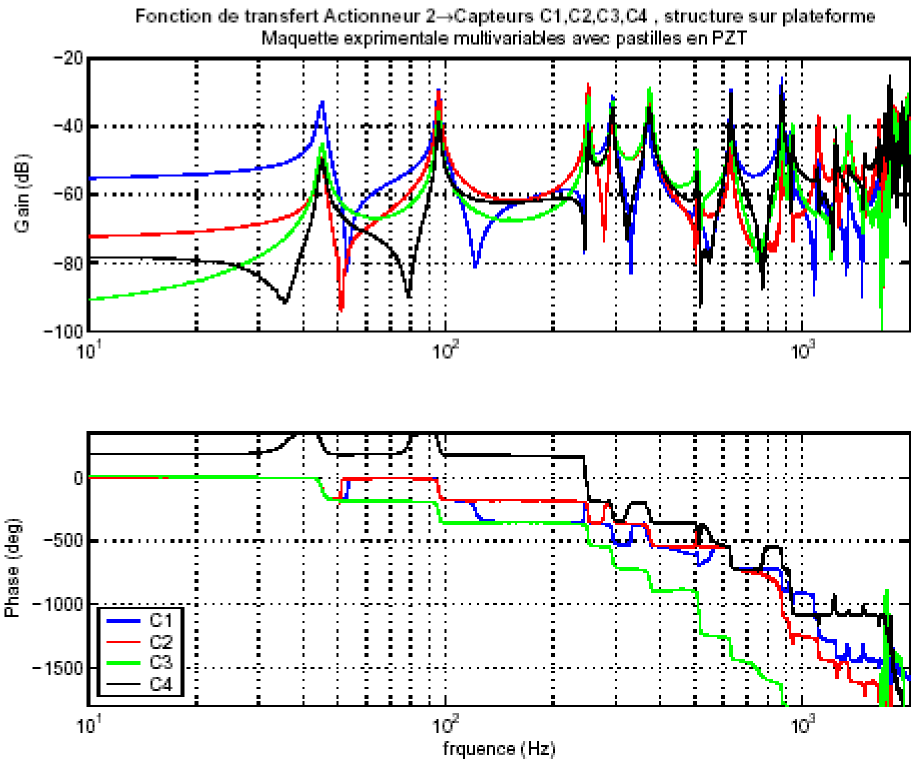

Comparaison simu./manip.

Cas de la plaque complexe

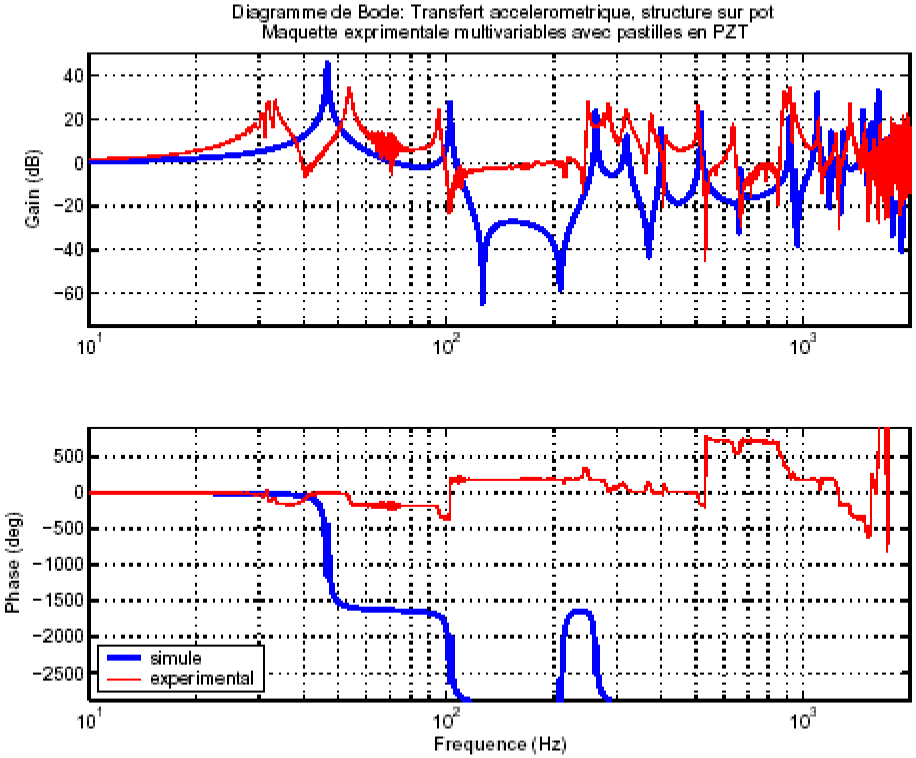

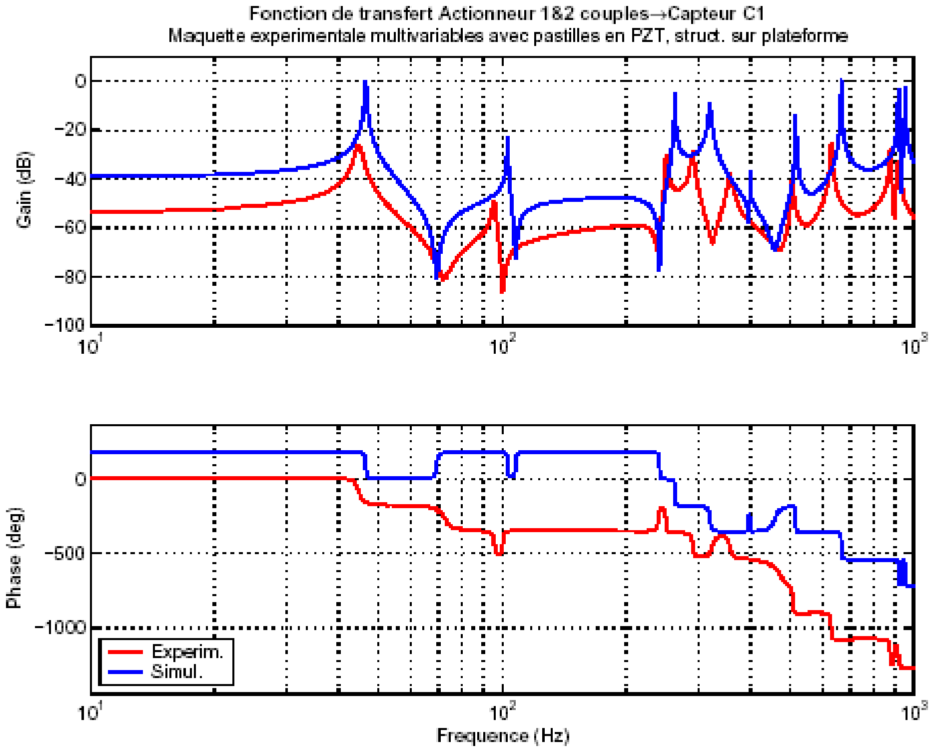

Comparaison simu./manip.

Cas de la plaque complexe

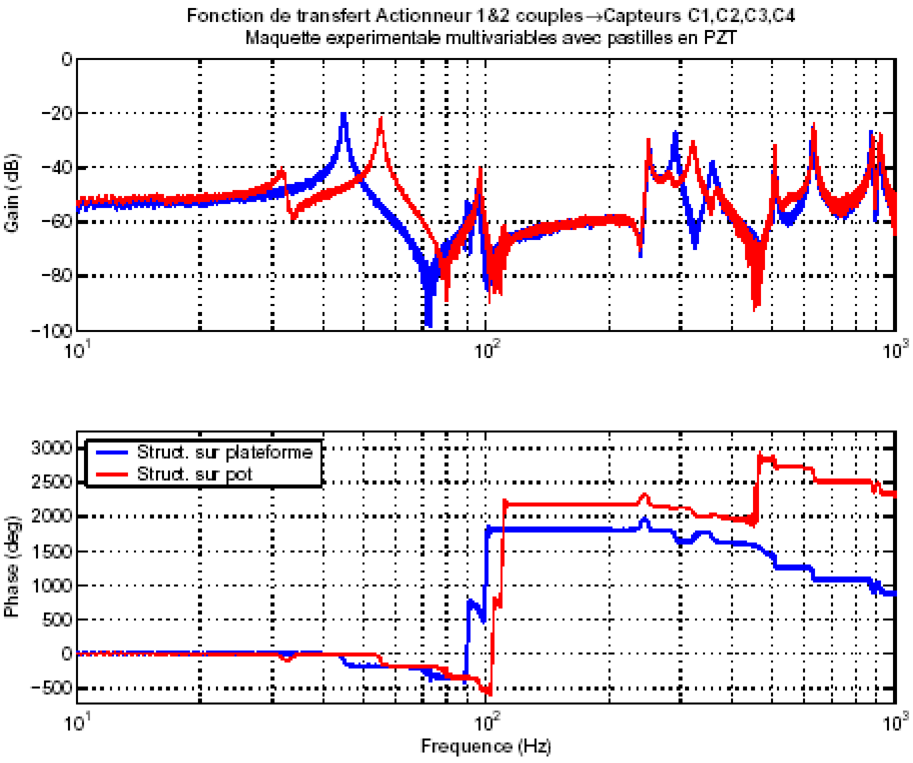

Problème de *couplage des structures* :

- Dynamique du pot
- Dynamique de la plaque

Commande robuste

Application au contrôle actif des vibrations

Cahier des charges

Critère de performance :

Atténuer le pic de résonance d'au moins 10 dB sur la réponse fréquentielle pot/accéléro,

Puissance spectrale imposée par le pot : ~10^{-3} g^2/Hz

Contraintes :

- Amplitude de commande limitée à +/-500V
- Garantir la stabilité robuste en boucle fermée
- Garantir un minimum de performances robustes
  - $\Rightarrow$ Dynamiques négligées
  - $\Rightarrow$ Incertitudes sur les fréquences (~10%) et amortissement propres (~30%)
- Complexité minimale (ordre, structure)

Formulation du problème de commande

Performances robustes $\rightsquigarrow$ Forme standard

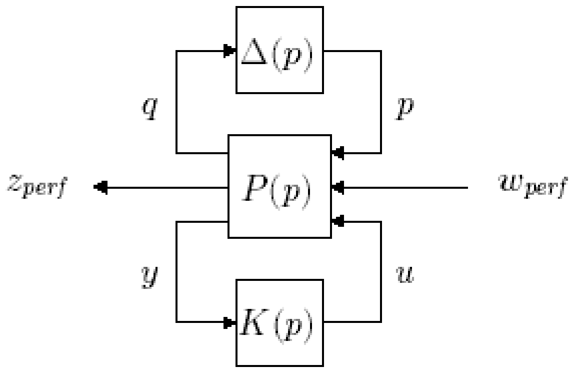

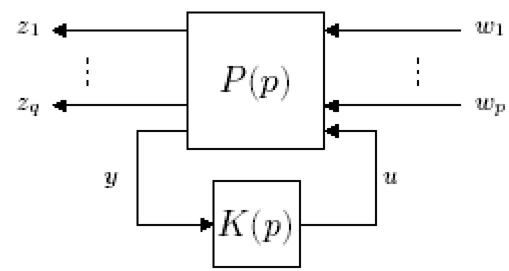

Synthèse H∞, H_2

Approche LMI,Riccati

- Signification physique du critère à minimiser
- Approche fréquentielle, réglage de pondérations
- Adapté à la prise en compte d'incertitudes
- Outils de synthèse monocritère : pessimiste

Références :

Apkarian, Gahinet, Chilali (1994)

Glover, Doyle, Zhou (1996) …

Schéma de synthèse

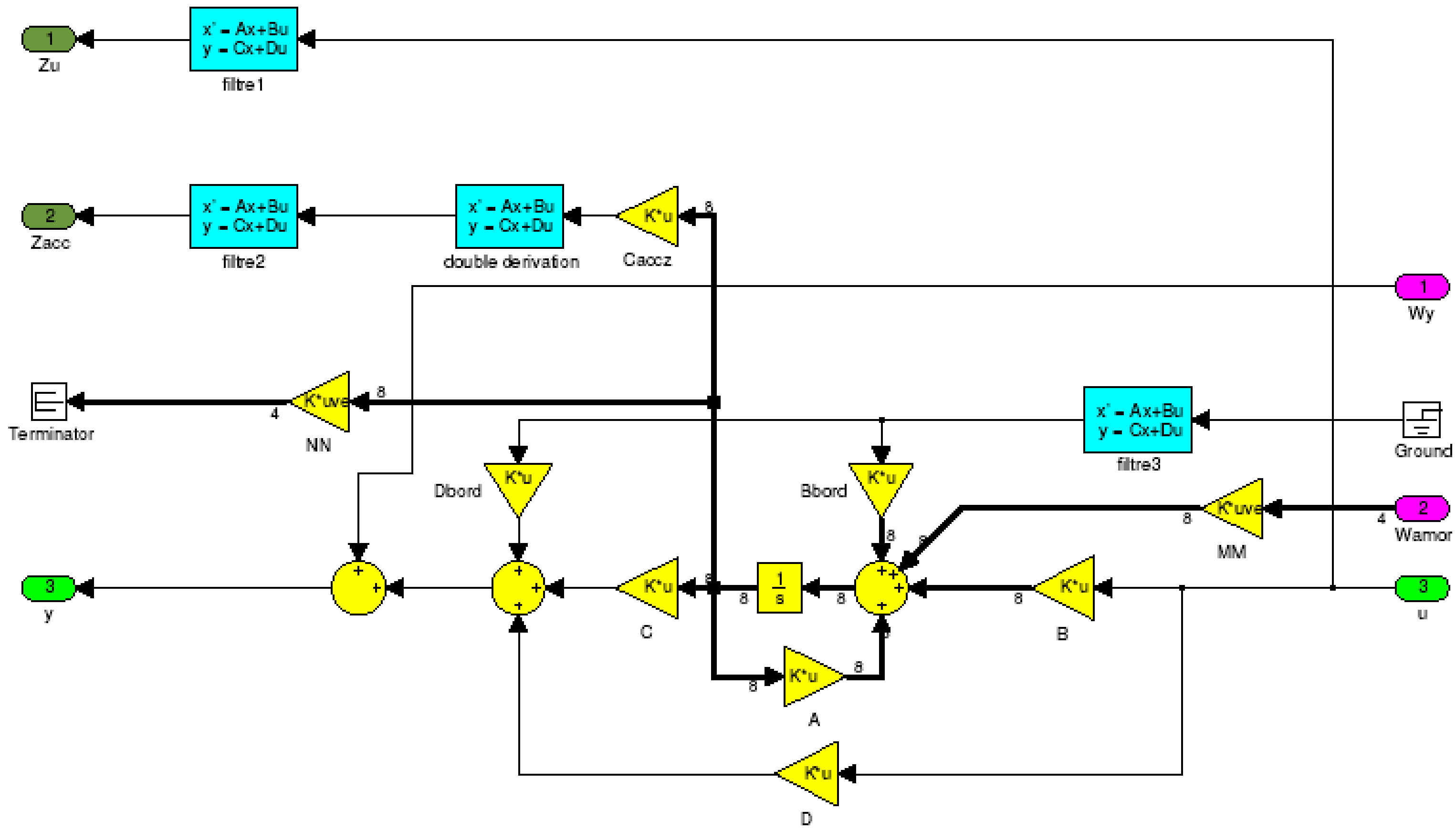

Réglage des pondérations

Cas de la plaque simple :

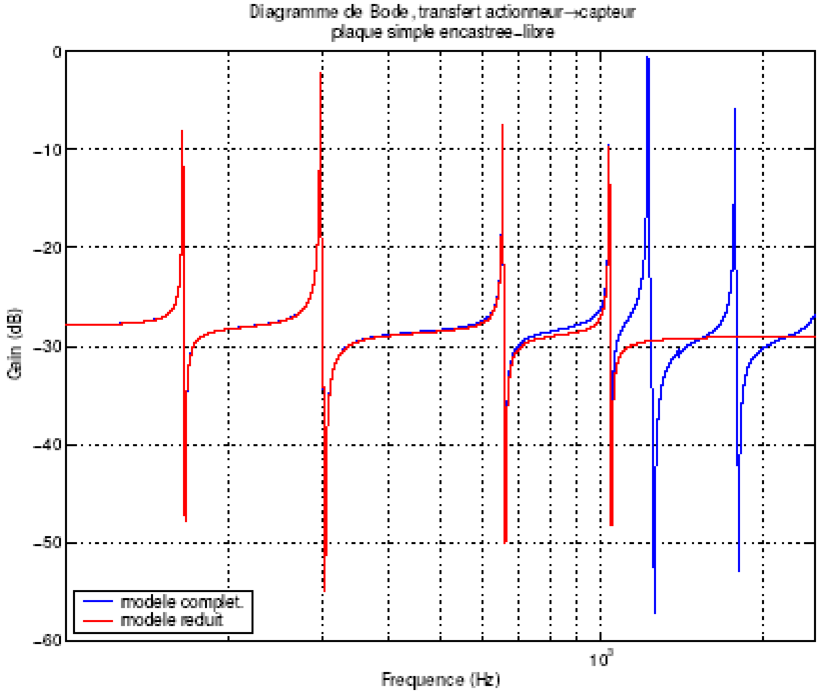

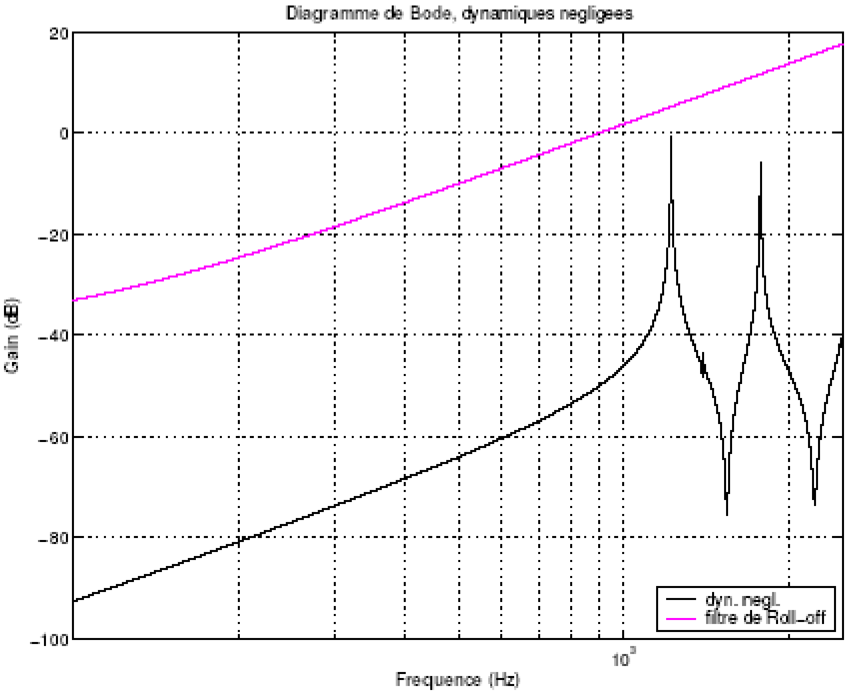

Résultats simulés

Cas de la plaque simple :

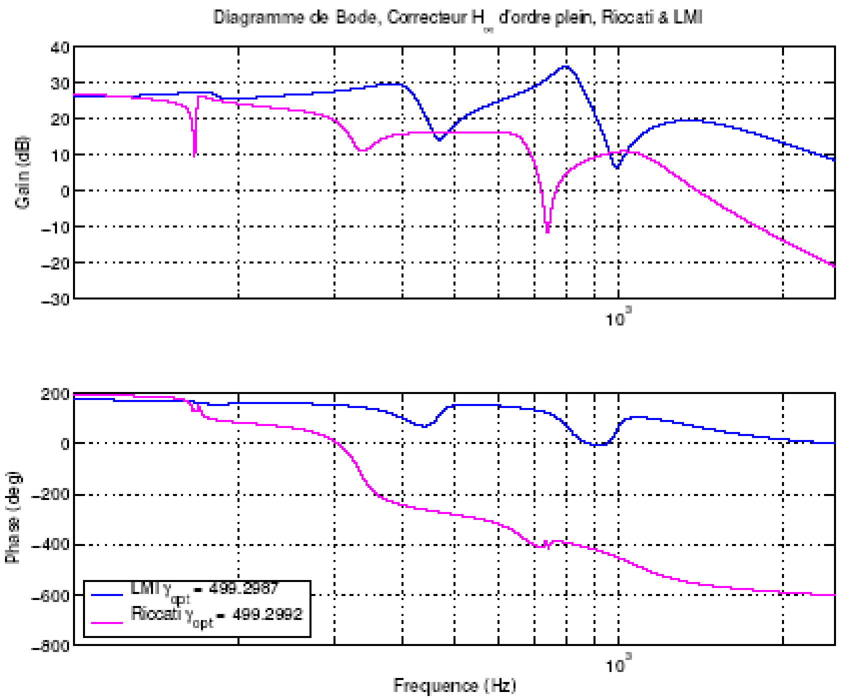

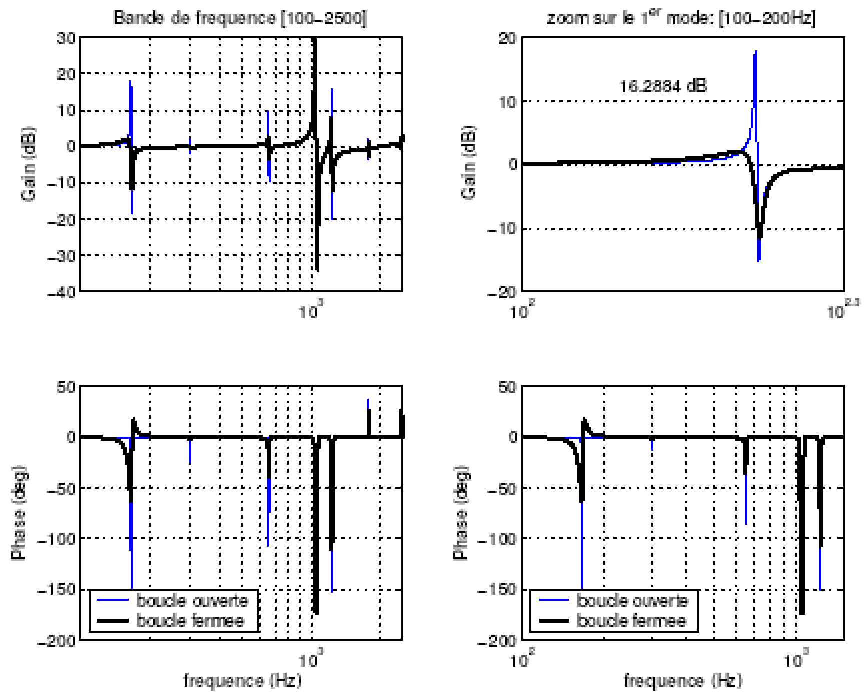

Résultats expérimentaux

Cas de la plaque simple :

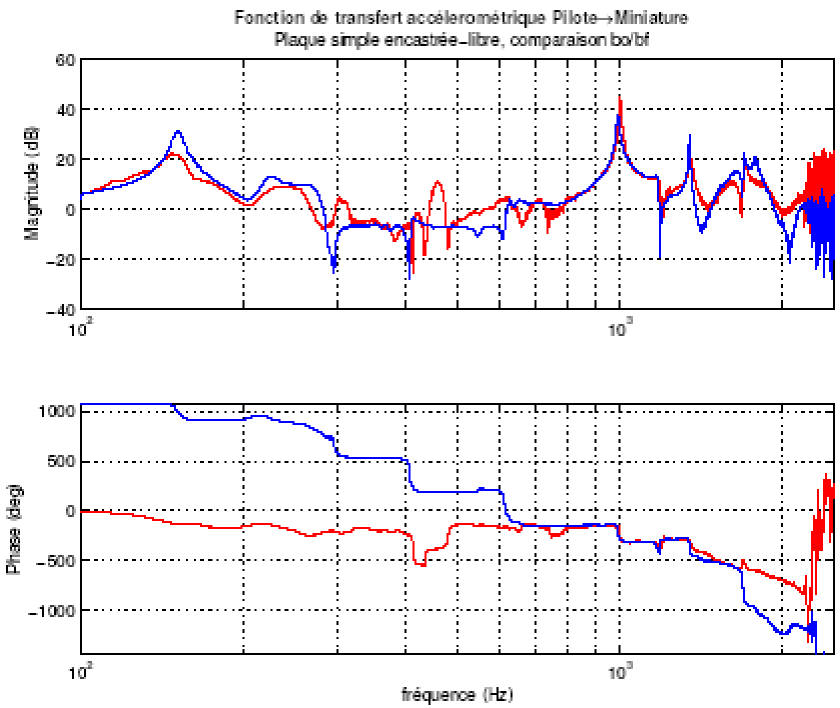

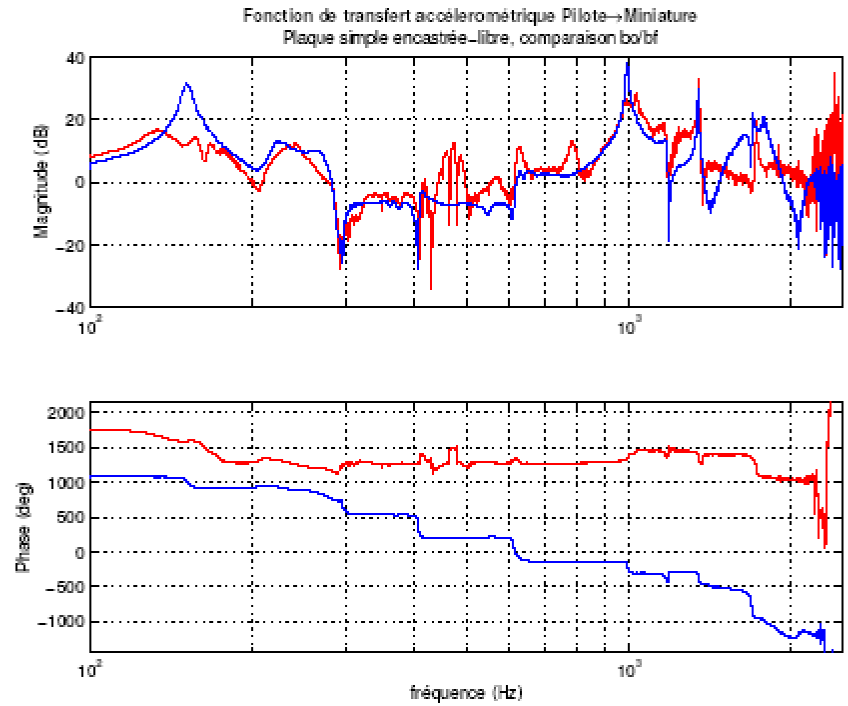

Bilan

Contrôle actif des vibrations :

Travail pluridisciplinaire :

- *Mécanique des structures, physique du matériau*
  - Formulation EDP, résolution numérique systématique
  - Modèle obtenu incertains
  - Non prise en comte des non-linéarités (hystérésis)
- *Automatique : problème de commande multiobjectif complexe*
  - Approche robuste : pessimisme
  - Lois de commande linéaire : saturation
- *Expérimentation en temps réel*
  - Besoin de nouvelle architecture d'implémentation : Complexité réduite
  - Implémentation de correcteurs non-linéaires/dim. ``infinie'' ?

Prospectives : commande à retard

Collaboration avec I. Boussaada, S.-I. Niculescu, en **dimension finie**

- Commandes à retard : correcteur QPB **[Boussaada & al, P. IUTAM 2018]**
- Approche spectrale,
- Paradigme MID,

Quid **dimension infinie** ? Nouvelle collaboration avec LAC-EDP, K. Ammari

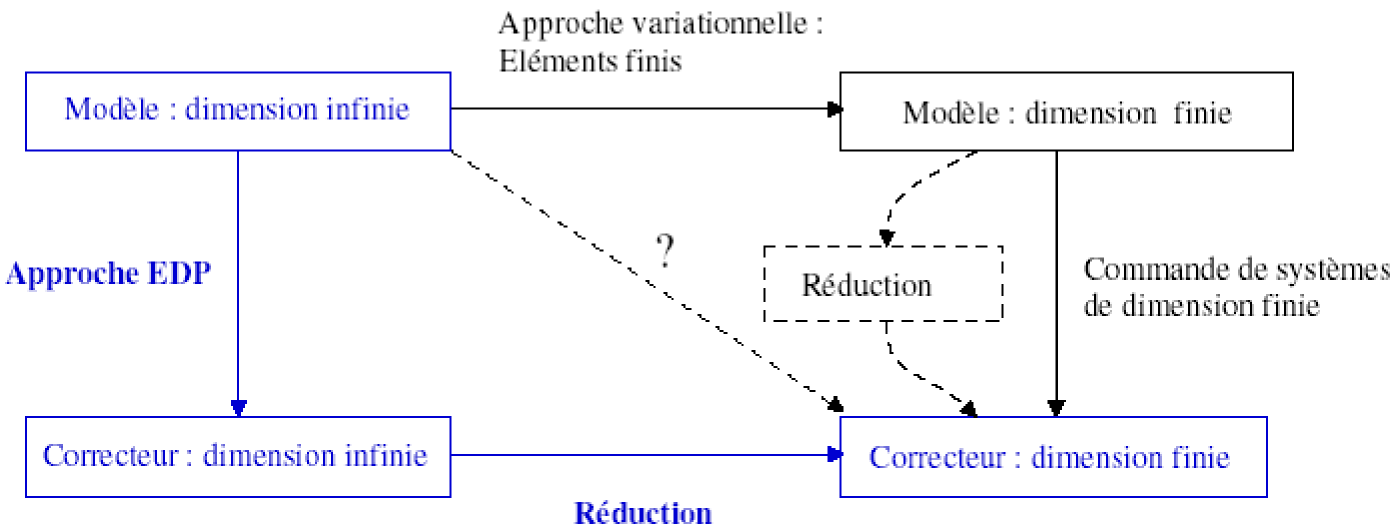

Design of Quasipolynomial-Based Controllers with Dynamical Parameters - Application to Active Vibration Damping

CTIP-2023, Control Theory & Inverse Problems, Monastir, Tunisia

Sami TLIBA* Islam BOUSSAADA Silviu-Iulian NICULESCU

*L2S Laboratoire des Signaux & Systèmes

Université Paris-Saclay, CNRS, CentraleSupélec

91190 GIF-SUR-YVETTE – France

Contact: sami.tliba@universite-paris-saclay.fr

May 8–10, 2023

Problem statement

Consider a linear time invariant (LTI) system $\mathscr{S}$, with control input $u(t) \in \mathbb{R}$, measured output $y(t) \in \mathbb{R}$, disturbance input $w(t) \in \mathbb{R}$ and controlled output $z(t) \in \mathbb{R}$, given in Laplace domain by

$$\mathscr{S} \begin{cases} Z(s) &= \dfrac{N_{wz}(s)}{\psi(s)} W(s) + \dfrac{N_{uz}(s)}{\psi(s)} U(s), \\ Y(s) &= \dfrac{N_{wy}(s)}{\psi(s)} W(s) + \dfrac{N_{uy}(s)}{\psi(s)} U(s), \end{cases} \tag{1}$$

where the polynomials, with real coefficients, have the form:

$$N_{ij}(s) := \sum_{k=0}^{n_p} n_{ij_k} s^k \quad \text{and} \quad \psi(s) := s^{n_p} + \sum_{k=0}^{n_p - 1} a_k s^k, \tag{2}$$

where $i \in \{u, w\}$ and $j \in \{y, z\}$ and n_p is the order of the system.

The control model, given by $\dfrac{N_{uy}(s)}{\psi(s)}$, is assumed to be in its minimal form, such that $N_{uy}(\cdot)$ and $\psi(\cdot)$ are co-prime polynomials.

Control objectives

Stabilizing unstable systems; Disturbance rejection; Trajectory tracking ...

⇒ Linear control problems are closely related to pole location in the complex plane.
Practical implementation of closed-loop controllers often requires output feedback.

⇒ This work is about the design of an **output feedback controller** achieving the following closed-loop control objectives:

- assign the dominant pole, complying with the desired transient dynamical behavior (stability, settling time, damping, ...),
- for experimental implementation requirements, the controller should :
  - have a low complexity (structure, required number of parameters),
  - be BIBO stable (satisfy the strong stability property).

Control objectives

$\Rightarrow$ Output feedback controllers with **delayed actions** happened to be relevant wrt the last two control objectives.

Main drawbacks: introduction of an **infinite number of poles**; hard to handle the closed loop dynamic with a finite number of parameters.

A solution : The **Partial Pole Placement** paradigm (**PPP**) *via* the **Multiplicity-Induced-Dominancy** (**MID**) property.

MID Property

Consider the dynamical system described by the *delay-differential equation (DDE)*:

$$y^{(n)}(t) + \sum_{k=0}^{n-1} a_k y^{(k)}(t) + \sum_{k=0}^{m} \alpha_k y^{(k)}(t-\tau) = 0, \tag{3}$$

under appropriate initial conditions, where $y(\cdot)$ is the real-valued unknown function, $\tau > 0$ is the delay, and $a_0, \ldots, a_{n-1}, \alpha_0, \ldots, \alpha_m$ are real coefficients.
Equation (3) is of *retarded type* if $m < n$, of *neutral type* if $m = n$.
Characteristic function associated to (3) is the quasipolynomial Δ given by

$$\Delta(s) := P_0(s) + P_\tau(s)\, e^{-\tau s}, \tag{4}$$

where P_0 and P_τ are the polynomials with real coefficients given by

$$P_0(s) = s^n + \sum_{k=0}^{n-1} a_k s^k, \quad P_\tau(s) = \sum_{k=0}^{m} \alpha_k s^k, \tag{5}$$

and the degree of Δ is the integer $\deg(\Delta) := n + m + 1$.

MID Property

A characteristic root $s_0 \in \mathbb{C}_-$ of Δ satisfies the *MID property* if

(i) its *algebraic multiplicity* $M(s_0)$ is *larger than one*,

(ii) it is *dominant*, *i.e.* $\forall \lambda_\sigma \in \mathbb{C} \mid \Delta(\lambda_\sigma) = 0$, the condition $\Re(\lambda_\sigma) \leq \Re(s_0)$ holds.

$\Rightarrow$ s_0 is the *rightmost root* of the spectrum and defines the *spectral abscissa* of the quasipolynomial Δ.

It was shown in [1] (case $m = n - 1$) and [2] (general case $m \leq n$) that,

Theorem (See [1],[2].)

if $M(s_0) = \deg(\Delta)$, then s_0 satisfies the MID property.

This "limit" case is also called *generic MID* (GMID).

[1](Mazanti, I. Boussaada, and Niculescu 2021)
[2](I. Boussaada, Mazanti, and Niculescu 2022)

The QPB controller structure

Consider the closed loop control structure with the standard QPB controller [3]

$$C(s,\tau) := \frac{n_0 + n_{\tau_0}\, e^{-\tau s}}{d_0 + d_{\tau_0}\, e^{-\tau s}} =: \frac{\mathcal{N}(s,\tau)}{\mathscr{D}(s,\tau)},$$

where τ, n_0, n_{τ_0}, d_0 and $d_{\tau_0} \in \mathbb{R}$. In time domain, the control law is:

$$u(t) = \underbrace{-\frac{d_{\tau_0}}{d_0}u(t-\tau)}_{\textit{auto-regressive term}} + \frac{n_0}{d_0}y(t) + \frac{n_{\tau_0}}{d_0}y(t-\tau),$$

based on proportional actions plus delayed proportional actions on y and u.

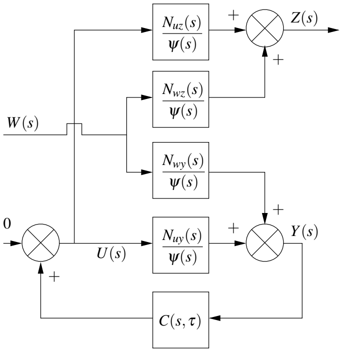

In practice, there are $N_P = 4$ independent parameters for the standard QPB controller: n_0, n_{τ_0}, d_{τ_0} and τ; $d_0 = 1$ for simplicity.

[3] Quasi-Polynomial Based controller, first introduced in (Islam Boussaada et al. 2017).

The closed loop features

The closed-loop relation between w and z is given by

$$Z(s) = \frac{N_{wz}\,\mathscr{D} + Q\,\mathscr{N}}{\psi\,\mathscr{D} - N_{uy}\,\mathscr{N}} W(s),$$

where $Q(s)$ is a polynomial of degree $\leq \deg \psi(s)$, such that

$$N_{uz}(s)\,N_{wy}(s) - N_{wz}(s)\,N_{uy}(s) = Q(s)\,\psi(s).$$

The corresponding characteristic function is given by

$$\Delta(s) := \psi(s)\,\mathscr{D}(s,\tau) - N_{uy}(s)\,\mathscr{N}(s,\tau),$$

$\Rightarrow$ a quasipolynomial that can be expressed as

$$\Delta(s) := P_0(s) + P_\tau(s)\,e^{-\tau s},$$

with $P_0(s) := d_0\,\Psi(s) - n_0\,N_{uy}(s)$ and $P_\tau(s) := d_{\tau_0}\,\psi(s) - n_{\tau_0}\,N_{uy}(s)$.

MID for Partial Pole Placement

Given a desired root $s_0 \in \mathbb{C}_-$ for the closed loop characteristic function $\Delta(s)$ (general case: $m \leq n$).

Main idea: force s_0 to be a root of $\Delta(s)$, of algebraic multiplicity $M(s_0)$, thanks to the N_P parameters of the standard QPB controller:

$\Rightarrow$ given $M(s_0)$, if the following conditions hold,

$$(n+1 \leq) M(s_0) \leq \deg(\Delta) \quad \text{and} \quad M(s_0) \leq N_P, \tag{6}$$

solve sequentially the set of equations

$$\Delta^{(k-1)}(s)\Big|_{s=s_0} = 0, \tag{7}$$

for $k = 1$ to $M(s_0)$ in the N_P controller's parameters, where $\Delta^{(j)}(s)$ stands for the j^{th} derivative of $\Delta(s)$ in terms of s.

Remark

It can be checked that the resulting set of equations in (7) are linear wrt the standard QPB's normalized parameters, excepting the delay τ.

MID for Partial Pole Placement

How the dominance of s_0 is ensured ?

- When $M(s_0) = \deg(\Delta)$, (GMID), the dominance of s_0 is guaranteed in the general case $m \leq n$ (neutral and retarded cases) as long as $M(s_0) \leq N_P$ is true. N_P depends on the the structure of the chosen controller.
  For example: with delayed actions, the designers use PID based control laws with up to 4 parameters, including the delay τ as a design parameter !
  Same amount of parameters N_P with the standard QPB controller.
- Problem: what happen if $N_P < M(s_0)$ or $(n+1 \leq)M(s_0) < \deg(\Delta)$ (*i.e.* if both conditions in (6) are not true) ?
  To overcome this situation:
  - A relaxation of the GMID case allows to release the constraints on the available N_P parameters: the dominance of s_0 is then not always guaranteed.
    $\Rightarrow$ A test of dominance is mandatory, as asserted and proposed in (I. Boussaada, Mazanti, Niculescu, and Benarab 2022).
  - increase N_P (change the controller's structure) until satisfying the second conditions (6) $\Rightarrow$ QPB controller with Dynamical Parameters;

Note: Changing N_P can lead to changing $\deg(\Delta)$!

MID for PPP: test of dominance

For the *intermediate algebraic multiplicity* case $M(s_0) = n + m < \deg(\Delta)$, an explicit integral representation of the quasipolynomial $\Delta(s)$ is given by the following theorem:

Theorem (I. Boussaada, Mazanti, Niculescu, and Benarab 2022)

Let $\tau > 0$, $s_0 \in \mathbb{R}$, and consider the quasipolynomial Δ from (4)–(5)*. The number s_0 is a root of Δ with multiplicity at least $n+m$ if, and only if there exists $A \in \mathbb{R}$ such that*

$$\Delta(s) = \frac{\tau^m (s-s_0)^{n+m}}{(m-1)!} \int_0^1 t^{m-1}(1-t)^{n-1}(1-At)e^{-t\tau(s-s_0)}\mathrm{d}t. \tag{8}$$

Detecting the roots of Δ with real part greater than s_0 is proposed *via* a procedure (algorithm) carrying on the *existence of an upper bound on the imaginary part for any root of Δ.*

MID for PPP: test of dominance

How to establish such a bound ?
Define $\tilde{\Delta}(\lambda) := \tau^n \Delta(s_0 + \frac{\lambda}{\tau})$.
It can be rewritten as $\tilde{\Delta}(\lambda) = \tilde{P}_0(\lambda) + e^{-\lambda}\tilde{P}_1(\lambda)$, where $\deg(\tilde{P}_0(\lambda)) = n$ and $\deg(\tilde{P}_1(\lambda)) = m$.
In that case: $\Re(s) \geq \Re(s_0) \Leftrightarrow \Re(\lambda) \geq 0$.

Define $\lambda := x + i\omega$. If $x \geq 0$, then $e^{2x} \geq T_\ell(x)$, where $T_\ell(x) := \sum_{k=0}^{k=\ell} \frac{(2x)^\ell}{\ell\,!}$.

Define $\mathscr{F}(x,\omega) := |\tilde{P}_\tau(x+i\omega)|^2 - |\tilde{P}_0(x+i\omega)|^2 T_\ell(x)$. Notice that $\mathscr{F}$ is a polynomial in ω^2 since $\tilde{P}_0(\lambda)$ and $\tilde{P}_1(\lambda)$ are real coefficient polynomials.
λ is a root of $\tilde{\Delta}$ if, and only if $|\tilde{P}_\tau(x+i\omega)|^2 = |\tilde{P}_0(x+i\omega)|^2 e^{2x}$.
If λ is a root of $\tilde{\Delta}$ with positive real part, then $\mathscr{F}(x,\omega) \geq 0\ \forall \omega \in \mathbb{R}$. This allows to bound ω^2 when λ is a root of $\tilde{\Delta}$ with positive real part.
As a consequence, it is shown that if $|\omega| \leq \pi$, then λ has a is a root of $\tilde{\Delta}$ with non-positive real part, meaning that s_0 is the rightmost root of Δ.

MID for PPP: test of dominance

How to establish such a bound ?
Define $\tilde{\Delta}(\lambda) := \tau^n \Delta(s_0 + \frac{\lambda}{\tau})$.
It can be rewritten as $\tilde{\Delta}(\lambda) = \tilde{P}_0(\lambda) + e^{-\lambda}\tilde{P}_1(\lambda)$, where $\deg(\tilde{P}_0(\lambda)) = n$ and $\deg(\tilde{P}_1(\lambda)) = m$.
In that case: $\Re(s) \geq \Re(s_0) \Leftrightarrow \Re(\lambda) \geq 0$.

Define $\lambda := x + i\omega$. If $x \geq 0$, then $e^{2x} \geq T_\ell(x)$, where $T_\ell(x) := \sum_{k=0}^{k=\ell} \frac{(2x)^\ell}{\ell\,!}$.

Define $\mathscr{F}(x,\omega) := |\tilde{P}_\tau(x+i\omega)|^2 - |\tilde{P}_0(x+i\omega)|^2 T_\ell(x)$. Notice that $\mathscr{F}$ is a polynomial in ω^2 since $\tilde{P}_0(\lambda)$ and $\tilde{P}_1(\lambda)$ are real coefficient polynomials.
λ is a root of $\tilde{\Delta}$ if, and only if $|\tilde{P}_\tau(x+i\omega)|^2 = |\tilde{P}_0(x+i\omega)|^2 e^{2x}$.
If λ is a root of $\tilde{\Delta}$ with positive real part, then $\mathscr{F}(x,\omega) \geq 0\ \forall \omega \in \mathbb{R}$. This allows to bound ω^2 when λ is a root of $\tilde{\Delta}$ with positive real part.

Remark

The procedure consists in increment ℓ by one at each iteration, where each step relies on finding an upper bound for ω^2 lower than π.

Dynamical QPB Controller: def.

Definition

The output feedback QPB controller with dynamical parameters is defined, in Laplace domain, by

$$D(s,\tau) := \frac{N_0(s) + N_{\tau_0}(s)\, e^{-\tau s}}{D_0(s) + D_{\tau_0}(s)\, e^{-\tau s}}, \tag{9}$$

where $N_0(s)$, $N_{\tau_0}(s)$, $D_0(s)$, $D_{\tau_0}(s)$ are polynomials in s with finite degree.
The total amount of available independent parameters, denoted N_P, is given by $N_P := \deg(N_0) + \deg(N_{\tau_0}) + \deg(D_0) + \deg(D_{\tau_0}) + 4$.

Remark

Note that the degrees of these polynomials are assumed to be such that all the following ***transfer functions*** *remain* ***proper*** *for practical purposes:* $F_y(s) := \frac{N_0(s)}{D_0(s)}$, $F_{y_d}(s) := \frac{N_{\tau_0}(s)}{D_0(s)}$ *and* $F_{u_d}(s) := \frac{D_{\tau_0}(s)}{D_0(s)}$, *with:*

$$\deg(N_0(s)), \deg(N_0(s)), \deg(D_{\tau_0}(s)) \leq \deg(D_0(s)). \tag{10}$$

Dynamical QPB Controller: prop.

Fact

The closed-loop system $\mathscr{S}$ *in* (1) *with the Dynamical QPB controller in* (9), *has the same characteristic equation than in* (4)

$$\Delta(s) = P_0(s) + P_\tau(s)\, e^{-\tau s}, \tag{11}$$

where now,

$$P_0(s) := D_0(s)\,\psi(s) - N_0(s)\,N_{uy}(s), \tag{12}$$

$$P_\tau(s) := D_{\tau_0}(s)\,\psi(s) - N_{\tau_0}(s)\,N_{uy}(s). \tag{13}$$

Moreover,

$$\begin{aligned} n &= \deg(D_0) + n_p, \\ m &= \deg(D_{\tau_0}) + n_p, \\ \deg(\Delta) &= \deg(D_0) + \deg(D_{\tau_0}) + 2\,n_p + 1. \end{aligned} \tag{14}$$

Dynamical QPB Controller: prop.

To summarize, with the Dynamical QPB controller :

- $\deg(N_0(s)), \deg(N_0(s)), \deg(D_{\tau_0}(s)) \leq \deg(D_0(s))$,
- $\deg(\Delta) = \deg(D_0) + \deg(D_{\tau_0}) + 2n_p + 1$,
- $N_P := \deg(N_0) + \deg(N_{\tau_0}) + \deg(D_0) + \deg(D_{\tau_0}) + 4$,

These relations allow to fulfill the requirement for an intermediate algebraic multiplicity $M(s_0) = \deg(\Delta) - 1$ with enough design parameters ($M(s_0) \leq N_P$), whatever the order n_p of the LTI system $\mathscr{S}$.

Some implementation insights

Denote by $f_{u_d}(t)$, $f_y(t)$ and $f_{y_d}(t)$ the inverse Laplace transform of $F_{u_d}(s)$, $F_y(s)$ and $F_{y_d}(s)$ respectively. In time domain, the control law derived from (9) reads:

$$u(t) := -f_{u_d}(t) * u(t-\tau) + f_y(t) * y(t) + f_{y_d}(t) * y(t-\tau), \tag{11}$$

where the symbol $*$ stands for the time domain convolution product of causal signals.

Remark

*$u(t)$ is the result of **filtered terms** carrying on $\mathbf{u}(\mathbf{t}-\tau)$ and $\mathbf{y}(\mathbf{t})$ as well as $\mathbf{y}(\mathbf{t}-\tau)$, that are all added.*
*Consequence: the complexity is slightly increased w.r.t. the standard QPB controller's one, but with the **benefit of a greater set of available degrees-of-freedom**.*

Some implementation insights

Remark

Note that the filters $F_{u_d}(s)$, $F_y(s)$ and $F_{y_d}(s)$ share the same poles. Each term of the control law (11) *can be filtered with a separate filter, i.e. each one with its own dynamic.*

Let us define the following proper linear transfer functions $G_{u_d}(s) := \frac{N_{u_d}(s)}{D_{u_d}(s)}$, $G_y(s) := \frac{N_y(s)}{D_y(s)}$, $G_{y_d}(s) := \frac{N_{y_d}(s)}{D_{y_d}(s)}$, and denote by $g_{u_d}(t)$, $g_y(t)$ and $g_{y_d}(t)$ their inverse Laplace transforms respectively.

In time domain, the control law of the generalized QPB controller with dynamical parameters is

$$u(t) = -g_{u_d}(s) * u(t-\tau) + g_y(t) * y(t) + g_{y_d}(t) * y(t-\tau) \tag{12}$$

Some implementation insights

The resulting controller derived from this control law expressed in the the Laplace domain leads to

$$U(s) = D(s,\tau)Y(s), \tag{13}$$

$$\text{where} \quad D(s,\tau) := \frac{G_y(s) + G_{y_d}(s)\, e^{-\tau s}}{1 + G_{u_d}(s)\, e^{-\tau s}}. \tag{14}$$

This last corresponds to a QPB controller with dynamical parameters as in (9), with

$$\begin{aligned} N_0(s) &:= D_{u_d}(s) N_y(s) D_{y_d}(s), \\ N_{\tau_0}(s) &:= D_{u_d}(s) N_{y_d}(s) D_y(s), \\ D_0(s) &:= D_{y_d}(s) D_y(s) D_{u_d}(s), \\ D_{\tau_0}(s) &:= N_{u_d}(s) D_y(s) D_{y_d}(s). \end{aligned}$$

The piezo-actuated beam system

System under consideration

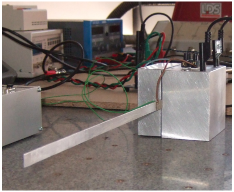

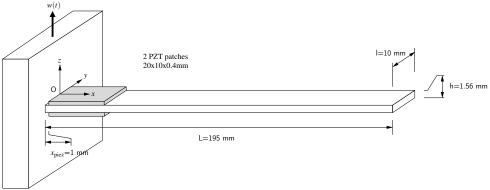

Flexible beam :

- clamped at one end, the other end is free,
- 2 piezo. patches bonded near the clamped end,
  - 1 actuator: require voltage $\phi^a \rightarrow$ induces mechanical strain
  - 1 sensor: deliver voltage $\phi^c \rightarrow$ measure of the mechanical deformation
- movable support submitted to perturbation $w(t)$: acceleration along axis z

The piezo-actuated beam system

System under consideration

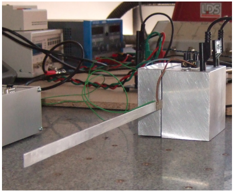

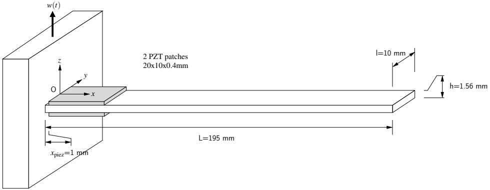

The model's mathematical feature:

- distributed parameter system
  - 1D case: 1 PDE Euler-Bernoulli equation $\frac{\partial^2}{\partial x^2}\left(E(x)I(x)\frac{\partial^2 q(x,t)}{\partial x^2}\right) + \rho\,\frac{\partial^2 q(x,t)}{\partial t^2} = \mathscr{F}(x,t)$, weak accuracy wrt experimental behavior,
  - 3D case: described by coupled PDEs in time and space variables,
- infinite dimensional system, complex topology, multiphysic.

$\Rightarrow$ Numerical modelling thanks to finite element method

Finite element based model

Meshing of the structure

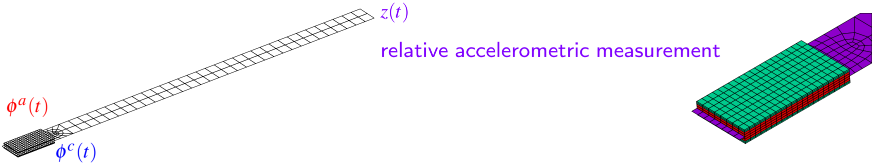

$$
\begin{aligned}
\mathbb{M}_{uu}\ddot{q}(t)\underbrace{+(\mathbb{D}_{qq}\dot{q}(t))}_{\text{damping term}}+\mathbb{K}_{qq}q(t) &= \mathbb{M}_{qw}w(t)-\mathbb{K}_{q\phi^a}\phi^a(t) && \rightarrow \textbf{eq. of motion}\\
\phi^c(t) &= \mathbb{K}_{q\phi^a}q(t) && \rightarrow \textbf{eq. of piez. sensor}\\
z(t) &= \mathbb{F}_{zw}w(t)-\mathbb{F}_{z\phi^a}\phi^a(t) && \rightarrow \textbf{eq. of free end}\\
& \quad -\mathbb{F}_{zq}q(t)-\mathbb{F}_{zv}\dot{q}(t) && \textbf{acceleration}
\end{aligned}
$$

- $w(t) \in \mathbb{R}$: (absolute) acceleration (m/s^2) of the movable support along axis z
- $z(t) \in \mathbb{R}$: relative acceleration (m/s^2) of the free end, derived from the equations of motion

Finite element based model

Meshing of the structure

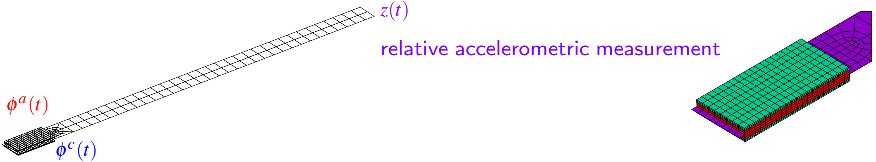

$$
\begin{aligned}
\mathbb{M}_{uu}\ddot{q}(t)\underbrace{+(\mathbb{D}_{qq}\dot{q}(t))}_{\text{damping term}}+\mathbb{K}_{qq}q(t) &= \mathbb{M}_{qw}w(t)-\mathbb{K}_{q\phi^a}\phi^a(t) && \rightarrow \textbf{eq. of motion}\\
\phi^c(t) &= \mathbb{K}_{q\phi^a}q(t) && \rightarrow \textbf{eq. of piez. sensor}\\
z(t) &= \mathbb{F}_{zw}w(t)-\mathbb{F}_{z\phi^a}\phi^a(t) && \rightarrow \textbf{eq. of free end}\\
& \quad -\mathbb{F}_{zq}q(t)-\mathbb{F}_{zv}\dot{q}(t) && \textbf{acceleration}
\end{aligned}
$$

- $\phi^a(t) \in \mathbb{R}$: piezo. actuator's voltage (control signal denoted $u(t)$ in the sequel),
- $\phi^c(t) \in \mathbb{R}$: piezo. sensor's voltage (measurement signal denoted $y(t)$ in the sequel),

Finite element based model

Meshing of the structure

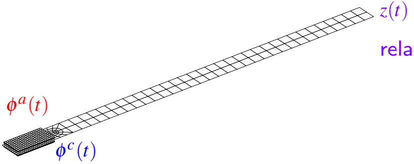

relative accelerometric measurement

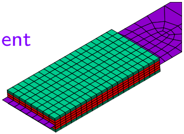

$$
\begin{aligned}
\mathbb{M}_{uu}\ddot{q}(t)\underbrace{+(\mathbb{D}_{qq}\dot{q}(t))}_{\text{damping term}}+\mathbb{K}_{qq}q(t) &= \mathbb{M}_{qw}w(t)-\mathbb{K}_{q\phi^a}\phi^a(t) && \rightarrow \textbf{eq. of motion}\\
\phi^c(t) &= \mathbb{K}_{q\phi^a}q(t) && \rightarrow \textbf{eq. of piez. sensor}\\
z(t) &= \mathbb{F}_{zw}w(t)-\mathbb{F}_{z\phi^a}\phi^a(t) && \rightarrow \textbf{eq. of free end}\\
&\quad -\mathbb{F}_{zq}q(t)-\mathbb{F}_{zv}\dot{q}(t) && \textbf{acceleration}
\end{aligned}
$$

- $\mathbb{M}_{qq}$, $\mathbb{M}_{qw}$, $\mathbb{K}_{qq}$, $\mathbb{K}_{q\phi^a}$, $\mathbb{K}_{q\phi^c}$, $\mathbb{F}_{zw}$, $\mathbb{F}_{z\phi^a}$, $\mathbb{F}_{zq}$ and $\mathbb{F}_{zq}$ are F.E.-matrices such that $q(t) \in \mathbb{R}^{\#5000}$!!! (#5000 degrees of freedom) $\Rightarrow$ model reduction is necessary.

Finite element based model

Reduction based on modal projection

The (vibrating) modes are the eigenvalues and the corresponding eigenvectors of the generalized eigenvalue problem:

$$\mathbb{M}_{uu}\lambda_i \varphi_i = \mathbb{K}_{qq}\varphi_i \quad i = 1 \dots n,\ \mathbb{M}_{uu} \succ 0,\ \mathbb{K}_{qq} \succeq 0$$

- Each eigenvalue $\lambda_i > 0$ give the eigenfrequency ω_i of a resonant mode.
- The corresponding eigenvector φ_i give the mode's shape associated with the resonant mode.

The Krylov algorithm is used to compute the n first eigenstructures in the ascending frequency order.

A modal basis is then derived $\Phi = \begin{bmatrix} \varphi_1 & \dots & \varphi_n \end{bmatrix}$ and used to perform a projection $q(t) = \Phi\xi(t)$ ($\xi(t) \in \mathbb{C}^n$, modal coordinates) of the motion and output equations along this new basis.

Finite element based model

Modal analysis

First in-plane bending modes:

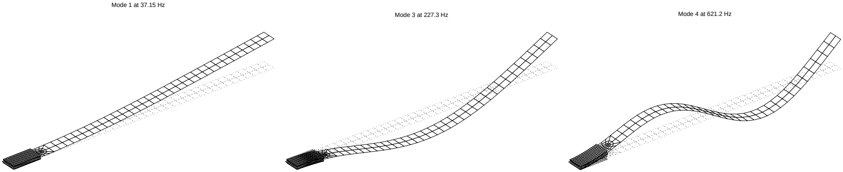

All controllable and observable

Finite element based model

Modal analysis

Next 3 in-plane bending modes:

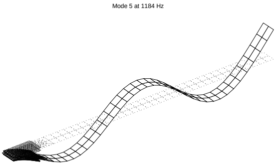

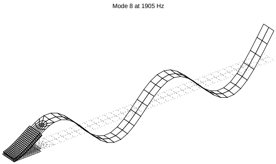

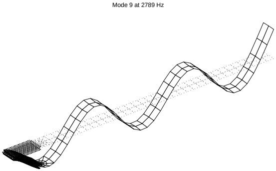

All controllable and observable

Finite element based model

Modal analysis

Other modes:

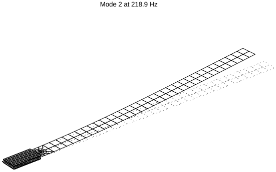

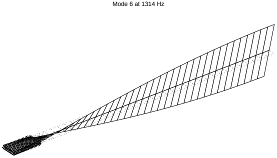

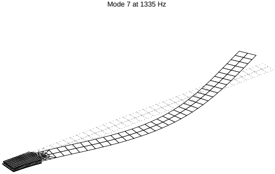

All not controllable **and** not observable

Finite element based model

For **analyze** purposes, we need a model:

- describing accurately the inputs-to-outputs dynamical behavior at low frequencies
  Bandwidth of interest: $[0 \quad 1500Hz]$
- of low order: reduce the computation burden during simulations

For **synthesis** purposes, we need a model:

- including the dynamics to control: first bending mode
- of order lower than the analysis model

The synthesis model is a reduced order model, derived from the analysis model by truncation and static gain preservation.

Finite element based model

Model derived from F.E. eq. of motion, in state-space form (*using standard notation in control theory*):

$$\mathscr{P}\begin{cases} \dot{x}_p(t) = A_p x_p(t) + B_{p,w} w(t) + B_{p,u} u(t) \\ z(t) = C_{p,z} x_p(t) + D_{p,zw} w(t) + D_{p,zu} u(t) \\ y(t) = C_{p,y} x_p(t) \; (+ D_{p,yw} w(t) + D_{p,yu} u(t)) \end{cases}$$

$x_p \in \mathbb{R}^{n_p}$ ($\xi = T x_p$, where $T \in \mathbb{C}^{n_p \times n_p}$ is an invertible matrix), $u \in \mathbb{R}$, $w \in \mathbb{R}$, $y \in \mathbb{R}$, $z \in \mathbb{R}$.

- n_p is 12 for analysis model
- n_p is 2 for synthesis model

Finite element based model

The synthesis state-space model is converted into a *transfer function* based model:

$$\mathscr{P}\begin{cases} z(s) = \dfrac{N_{wz}(s)}{\psi(s)}w(s) + \dfrac{N_{uz}(s)}{\psi(s)}u(s) \\ y(s) = \dfrac{N_{wy}(s)}{\psi(s)}w(s) + \dfrac{N_{uy}(s)}{\psi(s)}u(s) \end{cases}$$

$N_{wz}(s) = \sum_{k=0}^{n_p} n_{wz_k} s^k$, $N_{uz}(s) = \sum_{k=0}^{n_p} n_{uz_k} s^k$, $N_{wy}(s) = \sum_{k=0}^{n_p} n_{wy_k} s^k$, $N_{uy}(s) = \sum_{k=0}^{n_p} n_{uy_k} s^k$

and $\psi(s) = \sum_{k=0}^{n_p} a_k s^k$, where $a_{n_p} = 1$.

n_{wy_2}	-0.047734919434071	n_{uy_2}	0.0824705565013658
n_{wy_1}	-0.023286787751722	n_{uy_1}	0.0402320642368774
n_{wy_0}	-24664.7202708044	n_{uy_0}	5472.41008648971
n_{wz_2}	-1.57233229405836	n_{uz_2}	0.0407589609440159
n_{wz_1}	-0.767039493121702	n_{uz_1}	0.019883667632349
n_{wz_0}	0.114505932957013	n_{uz_0}	-0.00264721568397969
a_1	0.487835488732404	a_0	59495.8660165543

Finite element based model

Frequency responses on Bode-diagram

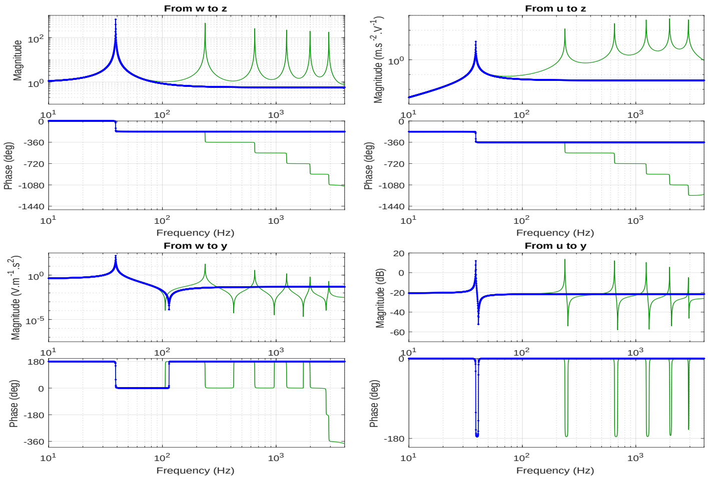

Control objectives

We seek for an output feedback controller achieving the following control objectives:

- reduce the peaks of resonance of the first bending mode ($\simeq 30\ dB$),

- guarantee the robust stability of the uncontrolled modes, prevent the spillover phenomenon due to the control signal at high frequencies,

- limit the controller's complexity, for (future) experimental implementation requirements,

- verify the strong stability property (BIBO stable controller).

Controller design

Choice is made to use a first-order filter combined with a QPB controller, with a low-frequency unitary gain but with a cutoff frequency let free for the design procedure.

$\Rightarrow$ the dynamical QPB controller in (9), $D(s,\tau) = \frac{N_0(s)+N_{\tau_0}(s)\,e^{-\tau s}}{D_0(s)+D_{\tau_0}(s)\,e^{-\tau s}}$ is sought with $D_0(s) := d_0\,(1+\alpha\,s)$, $D_{\tau_0}(s) := d_{\tau_0}$, $N_0(s) := n_0$ and $N_{\tau_0}(s) := n_{\tau_0}$.
It has $N_P = 5$ independent parameters: α, d_{τ_0}, n_0, n_{τ_0} and τ.

The resulting polynomials of the system's characteristic function $\Delta(s)$ in (4) are:

$$\begin{aligned} P_0(s) &= \alpha\,d_0\,s^3 + ((1+\alpha\,a_1)d_0 - n_0\,n_{uy_2})\,s^2 \\ &\quad + ((a_1+\alpha\,a_0)\,d_0 - n_0\,n_{uy_1})\,s + d_0\,a_0 - n_0\,b_{uy_0}, \\ P_\tau(s) &= \left(d_{\tau_0} - n_{\tau_0}\,n_{uy_2}\right)s^2 + \left(d_{\tau_0}\,a_1 - n_{\tau_0}\,n_{uy_1}\right)s \\ &\quad + \left(d_{\tau_0}\,a_0 - n_{\tau_0}\,n_{uy_0}\right). \end{aligned}$$

Note: By choosing d_0 such that $d_0\,\alpha = 1$, the coefficients of P_0 and P_τ are linear wrt the remaining design parameters, excepting the delay τ.

Solving procedure

$$\left\{ \Delta^{(k-1)}(s)\Big|_{s=s_0} = 0, \qquad \text{for } k = 1 \text{ to } M(s_0). \right.$$

Notice that $\Delta(s)$ is here of retarded type with $m = 2$ and $n = 3$, thanks to the presence of the first-order filter.

Let $s_0 \in \mathbb{R}_-$ be the multiple root to be assigned. The total amount of independent parameters to be tuned is $N_P = 5$.

The targeted multiplicity is $M(s_0) = n + m = 5$ (intermediate algebraic multiplicity), in order to assign freely s_0 while giving enough equations to deal with the number N_P of design parameters.

This set of equations is solved sequentially: s_0 is let free $\Rightarrow$ $s_0(\tau)$!

Numerical results

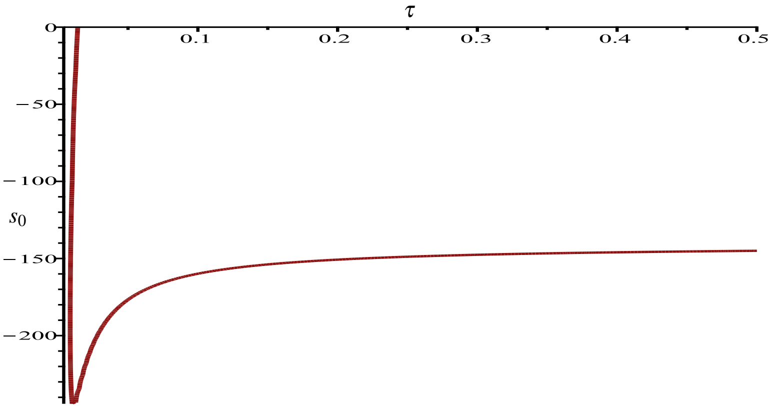

Figure: Admissible (s_0, τ) pair.

Numerical results, case $s_0 = -220$

Table: Dynamical QPB's parameters, $s_0 = -220$.

$n_0 \approx 10182.71$	$n_{\tau_0} \approx -7611.07$	$\tau \approx 8.9366 \cdot 10^{-3}$
$d_0 \approx 895.519$	$d_{\tau_0} \approx -637.158$	$\alpha \approx 1.1167 \cdot 10^{-3}$

Notice that $\left|\frac{d_{\tau_0}}{d_0}\right| < 1$,
$\Rightarrow$ the controller is BIBO-stable in open-loop.
The roll-off filter's cutoff frequency is roughly equal to $142.5\ Hz$, located at the right frequency region.

Figure: Closed loop spectrum

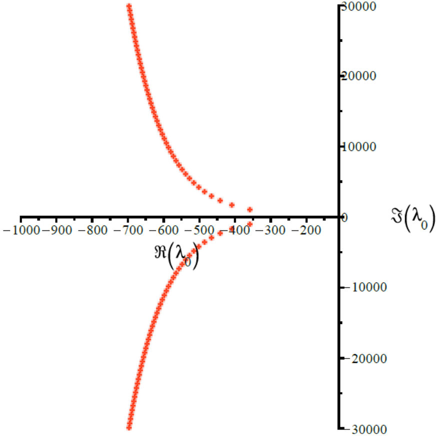

Numerical results, case $s_0 = -220$

Open (blue) *vs* closed-loop (red) simulations.

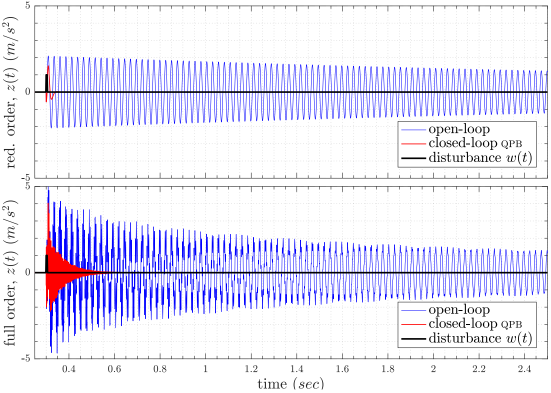

Figure: Time responses of the controlled output z, for the design model (top) and the full order model (bottom).

Numerical results, case $s_0 = -220$

Open (blue) *vs* closed-loop (red) simulations.

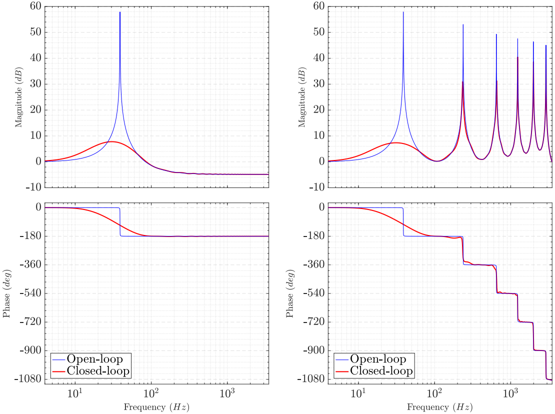

Figure: Accelerometric frequency responses of the w-to-$(w+z)$ transfer function, for the design model (left) and the full order model (right).

Conclusions

A "new" controller structure and its design procedure for finite dimensional LTI systems.
Some experimental/practical purposes have been taken into account thanks to:

- an **output feedback controller**,
- of **low complexity** since based on filtered plus delayed and filtered actions, with linear filters.

Our method is based on the right-most root assignment approach *via* **MID paradigm** and **QPB controller** with **dynamical parameters**.

This method was illustrated through the problem of active vibration damping of a perturbed piezo-actuated beam.

Conclusions

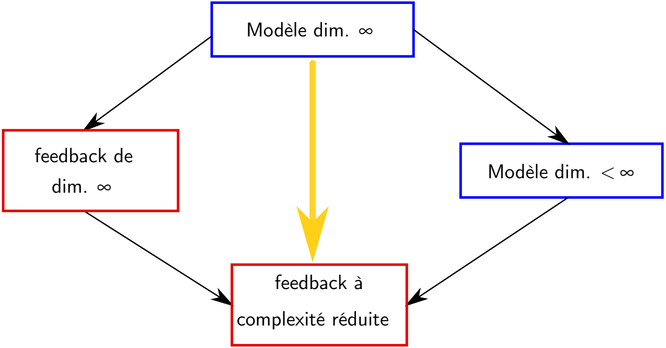

Thank you for your attention. . .

. . . merci pour votre attention.